AD NUMBER

AD911469

NEW LIMITATION CHANGE

TO

Approved for public release, distribution unlimited

FROM

Distribution authorized to U.S. Gov't. agencies only; Test and Evaluation; 03 MAY 1973. Other requests shall be referred to Commander, Naval Air System Command, Washington, DC.

AUTHORITY

USNA ltr, 4 Oct 1973

STRENGTHENING
of
Fe-Cr-Al-Y OXIDATION RESISTANT ALLOY

Final Report

(6 April 1972 to 6 April 1973)

Prepared Under Naval Air Systems

Command Contract No. N00019-72-C-0271

By

R. E. Allen

and

R. J. Perkins

6 May 1973

MATERIAL AND PROCESS
TECHNOLOGY LABORATORIES

AIRCRAFT ENGINE GROUP

LYNN, MASSACHUSETTS/CINCINNATI, OHIO

GENERAL ELECTRIC

FOREWORD

This is the Final Report for Contract N00019-72-C-0271, Department of the Navy, Naval Air Systems Command. The work covered in this report was completed during the period 6 April 1972 to 6 April 1973 and is an extension of work done under previous NASC contracts beginning 1 January 1971. These investigations were performed by the Material & Process Technology Laboratories (M&PTL) of the General Electric Company.

The Project Engineer for the Department of the Navy is Mr. I. Machlin. The Principal Investigator for this program is Dr. R. E. Allen, with Dr. C. A. Bruch as Program Manager.

ABSTRACT

An investigation of oxide dispersion strengthening (ODS) of oxidation resistant FeCrAlY alloys was conducted using argon atomized prealloyed powders and a modified SAP technique. The main objectives were to: improve surface stability; establish uniform powder pre-oxidation techniques; and improve the stress-rupture properties to the level exhibited by TD NiCr sheet. Increased chromium content proved very successful in eliminating "breakway" oxidation. Several powder pre-oxidation techniques were identified which provide uniform oxidation and prevention of nitrogen contamination. Target weight gains were consistently achieved. Rupture stress of the ODS FeCrAlY bar was raised to the 9.0 ksi level through the addition of 6 v/o oxide and is now comparable in strength to TD NiCr at temperatures above 2000F. If a density correction is applied to the rupture stress, ODS FeCrAlY is superior to TD NiCr at temperatures above approximately 1800F.

TABLE OF CONTENTS

1. INTRODUCTION

The objective of this program was the development of combined properties of strength, ductility and oxidation resistance in the FeCrAlY alloy system at temperatures in the 2000°F to 2500°F range. This system was selected because many of the alloys possess excellent surface stability (oxidation hot corrosion resistance) although they normally have poor mechanical properties at these temperatures. The principle task then was to improve structural properties without degrading surface stability. These improvements were sought by oxide dispersion strengthening.

Previous effort in this program (1, 2, 3) has centered around the oxide dispersion strengthening of two matrix chemistries Fe-25Cr-4Al-1Y (Alloy 2541) and Fe-15CR-5Al-1Y-1Cb (Alloy 1551-1Cb). Oxide additions were made by the SAP technique; i.e. pre-oxidation of atomized powder followed with densification by extrusion. Large elongated interlocking textured grain structures were achieved in both alloys by controlled thermo-mechanical sheet rolling processes.

Static oxidation resistance of Alloy 2541 and Fe-15Cr-5Al-1Y (Alloy 1551) was not affected by the addition of 1 to 4 v o oxide. A thin tightly adherent oxide film was formed and no intergranular attack, no internal oxidation and no depleted region was observed in static cyclic exposures of 2000°F 500 hours and 2400°F 100 hours. In addition, static air oxidation kinetics of ODS Alloy 2541 were not accelerated by exposure to 2100°F Mach 1 gases for 100, one-hour cycles.

The 1971 program consisted of two parts: one a partial scale-up of the best 1970 process and the second, an investigation aimed at increasing high temperature properties. The scale-up effort was for production of 12" wide sheet of Fe-15Cr-6Al-2Y (1562) . 4 v o oxide. Properties of this sheet were higher than were obtained during the 1970 program (N00019-70-C-0232) on small samples. In addition, longitudinal and transverse properties of the 12" wide sheet were nearly equivalent and were higher than TD NiCr transverse sheet properties at Larsen Miller parameters above 72 (C 25) as shown in Figure 1. In the investigation aimed at increasing properties it was found that the rupture stress of ODS FeCrAlY bar was almost 80 percent higher than that observed in sheet. A graphical comparison of TD NiCr sheet and ODS FeCrAlY bar is given in Figure 2.

Long time (10, 000 hours) hot corrosion testing at 1600°F and 1800°F indicates that ODS FeCrAlY is extremely resistant to attack and is far superior to any commercial nickel or cobalt base alloy.

In order to widen the range of potential application, further strengthening was being sought in the program described here. The best alloy produced to date represented an improvement of more than 20 times the 1000-hour rupture stress of the base Alloy 2541. This was achieved with no degradation of oxidation resistance. The goal of this program was to obtain an additional 50 percent strength increase in FeCrAlY alloys also without degradation of surface stability. This was attempted in a processing study aimed at refining procedures and chemistry of FeCrAlY alloys.

2. PROCESS DEVELOPMENT

2.1 POWDER PROCUREMENT

Three alloy chemistries of -325 mesh argon atomized powder were purchased from Alloy Metals, Inc. Nominal chemistries of these alloys in weight percent were: (1) 15Cr, 6Al, 2Y (Alloy 1562); (2) 20Cr, 6Al, 2Y (Alloy 2062); and, (3) 25Cr, 6Al, 2Y (Alloy 2562). Atomization was conducted from an induction melt of virgin material and atomization nozzle parameters were adjusted to give a high yield of -325 mesh powder. Chemical analysis of these three powders are shown in Table I. The oxygen level shown is higher than normal for argon atomization and is attributed to the very fine particle size compared to normal gas atomized powders. Since the powders were to be preoxidized before extrusion, the high oxygen level was not anticipated to be deleterious.

2.2 POWDER PREOXIDATION

Oxide addition to these powders was accomplished by preoxidizing the powders as in the SAP technique. This was anticipated to produce a thin shell of Al_2O_3 on the surface of each spherical powder particle. Preoxidation of small quantities of powder in thin layers on a metal tray was conducted quite successfully in an earlier program [1]. When larger batches of powder were preoxidized in air, however, nitrogen contamination problems were encountered [3]. In order to avoid nitridation, a subsequent effort was conducted in pure oxygen. In this case layering effects of nonuniform oxygen concentration were found in the large powder batches. Not only was the oxidation nonuniform on a macro scale but when individual powder particles were examined, micro scale nonuniformities were observed. Subsequent analysis showed these to be related to the "break away" oxidation phenomenon reported in Ni, Co and Fe base MCrAl by Stott, et al [4]. The phenomenon was found [4] in alloys of the MCrAl family which were low in Cr content. Sporadic, rapid oxidation rates were observed in such alloys as a result of forming other oxides than the protective Al_2O_3 scale. In cases where break away oxidation was observed in FeCrAl, the outer scale formed Fe_3O_4. An inner scale of complex Cr_2O_3, Fe_3O_4, and Al_2O_3 oxides resulted from rapid internal oxidation. The occurrences of break away oxidation found previously in some 15% Cr FeCrAlY powders was thought to be attributable to the very high surface to volume ratio found in these powders. Thr formation of the thick oxide scale on powders was deleterious to the final oxide dispersion also, because such massive oxides carried over into the densified product where they appeared as very large stringers. In addition to their undesirable size and distribution, these clumps are expected to be unstable because they should be reduced by Al in solid solution to form Al_2O_3.

In order to eliminate these problems from the preoxidation step, a detailed study of powder preoxidation was undertaken in this program. Studies were performed to establish conditions for the preoxidation of the three compositions to 1 w/o and 2 w/o oxygen (4 and 8 v/o oxide). These included the determination of weight change as a function of powder compaction, temperature, time and powder depth. Small porcelain crucibles containing various depths of powder, ranging from 0.1" to 0.8" were placed in a tray and inserted in a glo-bar heated

box furnace. The powders were cooled, weighed and inspected for oxidation uniformity (based on color) at times of approximately 2, 4 and 20 hours. The results are shown in Tables II, III and IV. In the design of the experiment it was believed that it would be possible to determine a safe working powder depth by varying the powder level. However, as can be seen from the data (Table III) the 2062 alloy preoxidized at 1400°F and the 2562 alloy preoxidized at 1200°F (Table IV), the weight change vs. powder depth measurement does not appear to be sensitive enough to detect layering effects that were obvious by color changes. The deeper samples, 14, 15, 18, 41, 42 and 45 showed color transitions at 0.4" and 0.5".

Specimens of each composition were selected from the preoxidation studies and were evaluated for uniformity of oxidation. Analysis of the oxide formation was performed using a scanning electron microscope (SEM) and energy dispersion analysis x-ray (EDAX) equipment. The SEM/EDAX analysis and photos are shown in Figures 3, 4 and 5. Alloy 1562 (Spec. 7 of Table II) of Figure 3 which was preoxidized at 1100°F for 22 hours in air to 1.2 w/o oxygen appears to have some evidence of break away. Although not as severe as was observed in an earlier program[3], the lack of protective Al_2O_3 scale is illustrated in Figure 3 may be observed along with the appearance of the inner complex oxide scale normally observed during break away oxidation. The 2062 material (Spec. 26) of Table III oxidized at 1200°F for 20 hours in air, to 1.4 w/o and the 2562 (Spec. 43 Table IV) oxidized at 1200°F for 4.2 hours in air to 1.1 w/o showed no evidence of break away oxidation as shown in Figures 4 and 5 respectively.

The safe working depth of the preoxidation of FeCrAlY -325 mesh powder was determined to be approximately 0.3". Subsequently several preoxidation runs were performed in a common glo-bar heated box furnace using shallow trays approximately 12" square and a powder depth of 1/4". Information about these runs are shown in Table V. Using time-temperature parameters tailored for each FeCrAlY composition, this technique has demonstrated reliability in obtaining predicted weight gains of 1% and was used for the processing of pilot scale extrusion studies. Oxidation uniformity based on color was excellent. Vacuum fusion analysis for O_2 and N_2, both before and after furnace exposure, are shown in Table V. The oxygen contents determined by vacuum fusion are fairly consistent with weight change measurements made on small smaples which were exposed simultaneously in small porcelain crucibles. Past experience had indicated the weight change determinations to be more reliable than the vacuum fusion results but vacuum fusion results are becoming more accurate and precise with the combination of improved analytical procedures and more uniform preoxidation. No nitrogen contamination was observed in powder preoxidized at a 1/4" depth or less.

Two approaches that were more favorable for the production of large quantities were investigated. In one approach the preoxidation was conducted in a rotary kiln where fresh material was continuously exposed to the oxidizing environment. A five pound batch of Alloy 1562 was preoxidized in a gas fired calciner at Bartlett-Snow Corp., Cleveland, Ohio*. This resulted in a very uniform oxidation of the powder indicating that this approach should effectively eliminate the layering previously encountered in large batches. The five-pound batch was tumbled for six hours at a mean temperature of 1100°F. Temperature

*Bartlett-Snow Corp. manufactures calciners. They do not normally operate as a heat treat service function but were cooperative in this program in order to increase their technical background and in order to promote utilization of their equipment.

control was poor (1060° to 1200°F) and contamination from a coarse refractory-like substance was found throughout the powder. Since the contaminant was coarse, sieving through a -325 mesh screen seemed to be successful in separating the contaminant from the FeCrAlY. Semiquantitative spectrographic analysis conducted after screening showed no evidence of foreign material. Both visual examination of the powder and metallographic examination of the extruded billet indicated the preoxidation was very uniform. Chemical analysis of the powder before and after preoxidation is shown in Table VI.

An extensive search for an available clean rotary kiln proved unsuccessful. This technique is believed to be a good one but will be discontinued, at least temporarily until it becomes economically feasible to purchase or build equipment solely for FeCrAlY use.

The other scale-up approach was a "moving-tray" experiment. A five-pound batch of Alloy 2062 was preoxidized at the Electric Furnace Co., Salem, Ohio. Two shallow trays were moved through an electrically heated roller conveyor furnace system having a 12 foot long hot zone. The furnace exposure was 1175°F for 4 hours in air. Two small porcelain crucibles containing equivalent depths of powder were placed in each tray so weight gain determinations could be made.

The results were the same as obtained in the static tray runs. The target 1% weight gain was achieved and color change and uniformity was excellent. There was some evidence of a trace amount of furnace brick refractory deposit on the surface of the powder (also experienced in the static tray runs) but was easily removed from the sintered powder with a blast of air. Semiquantitative spectrographic analyses of the powder before and after preoxidation are shown in Table VII. Ultimately a solid conveyor belt feed by a hopper could be used. Both techniques offer good control and quantity.

2.3 EXTRUSION

Consolidation and primary TMP of the ODS FeCrAlY alloys were accomplished by extrusion. The preoxidized powders were blended in a twin shell blender to minimize any inhomogeneities that could have occurred and then loaded into mild steel extrusion capsules. Design of the capsule, shown in Figure 6, is 3" in diameter x ~ 8" long with a 1 8" to 1 4" thick wall. The 1/8" thick plates at each end are necessary to prevent gas leaking which could occur when using nose and tail materials made from slices from hot rolled steel bar. The continuous inclusion stringers in the hot rolled bar can act as a path for gas leakage.

Bulk density of the powder was increased to about 65% of theoretical by tapping on the side of the container while loading the powder. Assembly of the billet was accomplished by TIG welding. Final sealing was performed by EB welding a small hole at the rear of the can after an overnight (at least 16 hours) evacuation to 5×10^{-5} torr.

The FeCrAlY powder billets were extruded on a 700 ton press at Wright Patterson Air Force Base in Dayton, Ohio. The extrusions were pushed at 1650° to 1750°F at a 16:1 reduction in area to 3/4" diameter rod. Appearance of the rods was good. They were straight and had no external cracks. Sectioning the rods at several locations determined the FeCrAlY core to be sound and of good configuration: the cross section was round with a uniform mild steel jacket approximately 0.060" thick and there was no apparent variation in uniformity along the length.

Density of the FeCrAlY core averaged 7.034 gms cc. Theoretical density of the ODS FeCrAlY is unknown but metallographic examination indicated there was no porosity present.

The microstructures of the extruded 2062 and 2562 alloys can be seen in Figure 7. Transverse and longitudinal views are shown at 500 times their actual size. Both compositions have similar appearance. The originally spherical powder particles were reduced in cross sectional area and elongated by approximately 16 times by extrusion. Oxide particles formed during break-up of the preoxidized film on the periphery of the particles were strung out in the direction of extrusion. These prior particle boundary oxides which were formed at the low preoxidation temperatures then evidently reacted at higher temperatures with the yttrium in the powder to form a more stable and uniform dispersion. The origin of the relatively oxide free regions in the material are not understood but may be simply the largest size powder particles. These regions were prone to primary recrystallization and are believed to be degrading to the strength of the material. Scanning electron microscope analysis was unsuccessful in distinguishing any variation in chemistry from one particle to another. Yttrium content is low in these FeCrAlY alloys and is not readily detectable by SEM analysis even in the heavily dispersioned areas.

Subsequent to extrusion, the materials were heat treated at 2400°F for 2 hours and examined metallographically for exaggerated grain growth. Macro etching the FeCrAlY in HCL - H_2O_2 solution revealed no grain growth response. Therefore, secondary TMP working techniques were necessary to produce the desired large elongated grains.

2.4 ROD ROLLING

A rod rolling study was conducted to establish rolling temperature and amount of reduction necessary to produce the desired grain growth in a subsequent recrystallization treatment. Alloys 1562, 2062 and 2562 all containing 4 v o oxide were rod rolled at 1400°F to a total of 60% reduction in area. Rolling was performed with the FeCrAlY core still in the mild steel extrusion jacket. The material was reduced 10% each pass, rotating the rod 90° between passes. Attempts to rod roll the FeCrAlY without the mild steel jacket or inserting into stainless steel tubing proved unsuccessful. The alloy suffered surface cracking and recrystallized to a duplex grain structure; i. e., small grains near the surface and large near the center. The cladding helped to retain the heat and also acted as a lubricant which promoted a more uniform strain in the lateral direction. Small sections approximately 3/4" long were removed from the rod at 20 and 40% reduction levels.

All three reduction levels were heated at 2400°F for 2 hours to check for recrystallization response. Virtually all samples exhibited the desired growth. The results are shown photographically in Figure 8. The grain size varies as a function of percent reduction and chromium content. The higher the reduction, the smaller the grain size. The higher the chromium content the smaller the grain size.

Additional rod rolling experiments determined good recrystallization response for a 20% reduction could be achieved in Alloy 1562 by rolling at 1500°F, Alloy 2062 at 1550°F and Alloy 2562 at 1600°F. This resulted in a comparable grain size for all three compositions. The macrostructures of Alloy 2062 and 2562 specimens are shown in Figure 9. Grain size is large, has a high aspect ratio and good uniformity throughout the cross section.

3. EVALUATION AND DISCUSSION

3.1 THERMAL STABILITY STUDIES

Iron base alloys such as ferritic stainless steels, FeCrAl and FeCrAlY alloys are subject to low temperature aging effects. Two separate low temperature phases are involved, α' and σ. Alpha prime is the Cr-rich solid solution phase that precipitates at temperatures below 970°F. Sigma, a nearly equiatomic Fe-Cr phase occurs at temperatures below 1500°F. Both phases are brittle and can cause deleterious effects on ductility. Although aging studies have been conducted in cast and wrought FeCrAlY alloys, the influence of the oxide particles was unknown. Hence, several ODS alloys were prepared and aged to investigate the aging behavior of these alloys.

3.1.1 Low Temperature Aging Experiments

Powders of Alloys 2062 and 2562 were preoxidized to 1% weight gain and extruded at 1650F 16X in a single step. Three foot lengths of these materials were rod rolled as follows: 2062 + 4 v/o - 1550°F/20% reduction and 2562 + 4 v/o - 1600°F/20%. These rolling schedules were selected because they yield the same recrystallized grain size in each material. This rolled stock was cut into 6" lengths and directionally recrystallized (DR) at approximately 2500°F using 2 inches per hour rate of travel through a temperature gradient of approximately 300°F/inch. The resulting microstructures are shown in Figure 10. Grains approximately 1/8" in diameter traversed the entire length of the sample. Coin shaped specimens were cut from the 6" long bars and these, along with theremaining lengths or bar were used in the aging study. In addition to DR 2062 + 4 v/o and DR 2562 + 4 v/o, coin shaped specimens of cast and wrought Alloys 1541 and 2541 were also used in the study. In order to determine the influence of starting microstructure, as-rod-rolled specimens of Alloys 2562 + 4 v/o and 2062 + 4 v/o and as-extruded 1562 + 4 v/o were also exposed in the aging study. Chemistries of all starting materials are given in Table VIII.

Aging exposures were conducted in α' and σ regions of the phase diagram shown in Figure 11[1]. Rockwell C hardness measurements were taken on samples of all alloys after various exposure times at 842 and 1025°F. These data are shown graphically in Figures 12 and 13 and Tables IX and X. As is shown in the graphs, α' precipitation caused an appreciable increase in hardness. Exposure in the σ region at 1025°F on the other hand, produced only small changes in hardness. After 1000 hours exposure, the increase in hardness due to α' was largest in the 25% Cr alloys and varied directly with Cr content. Conventional cast and wrought alloys also showed this same effect of Cr on hardness after aging. The hardness increase experienced in 1000 hours at 842°F was larger in the conventional alloys than in the ODS alloys of comparable Cr content. Thus the ODS 2562 alloy showed an increase in R_C hardness of 14 while the 2541 alloy increased by 23. Alloys with 15% Cr showed the same trend; i. e., ODS 1562 increased by 10 while 1541 increased by 16 units of R_C hardness. Starting microstructure also played a role in hardness changes at 842°F as can be deduced from Table IX by comparing the data from DR and rod rolled specimens at constant Cr levels. Changes in hardness were largest in the large grained DR alloys. This may have

been due to concurrent recovery in the fine grained rod-rolled alloys since they contained stored energy from the rolling process.

Samples of each of the ODS alloys were taken after 500 hours aging at both α' and σ forming temperatures for use in a solutioning study. Solutioning of the precipitate formed during the 500-hour aging cycle was attempted at 1200°, 1300°, 1400° and 2000°F. Hardness after varying lengths of time at each of these temperatures is given in Tables XI and XII. These data reveal that a dramatic reduction in hardness occurs in specimens containing α' (aged at 842°F) after only 5 minutes exposure at temperatures as low as 1200°F. No additional decrease in hardness is observed after longer exposure times at 1200°F up to 1 hour.

This same trend is seen at both 1300°F and at 1400°F. After solutioning the α' at 1400°F for 17 hours, the hardness loss is the same as that seen after 1200°F 5 min. exposure. Furthermore, this hardness value is slightly higher than that of the unaged alloy, indicating that either another precipitate is forming or that the α' is not completely solutioned. When the solution exposure is increased in severity to 2000°F for 20 hours, the hardness returns to that of the alloy prior to aging.

Alloys which were aged in the σ region at 1025°F for 500 hours showed very little hardening. Increases of 1, 2 and 4 units of R_c hardness were observed in ODS Alloys 1562 and 2562 respectively. No change in these hardness values were obtained after solutioning for up to 1 hour at 1200° and 1300°F or at 1400°F for 17 hours. A solution treatment at 2000°F for 20 hours was again effective in reducing the hardness to its pre-age level.

Both the solutioning and aging temperatures are marked on the phase diagram of Figure 11 at the appropriate Cr content. The diagram shown is one of several presented by Williams [5]. The $\alpha + \alpha' + \gamma'$ phase boundary is modified for 4% Al contents according to Wukusick[6]. After aging at 842°F and solutioning at 1200°, 1300° and 1400°F, the specimen exhibited residual hardening which disappeared after 2000°F 20 hours exposure. Since these solutioning temperatures are outside the $\gamma + \sigma$ phase field, this residual hardening may not be attributable to σ formation. Grobner[7] reported slight hardening in an Fe-18Cr alloy after aging at 1000°F which he attributed to the formation of $Cr_{23}(C, N)_6$. Although the ODS alloys are low in C and N, (~.02% total) the total volume fraction of carbonitrides that could form is approximately 0.4 v/o and this amount of precipitate could cause the observed hardening. ODS alloys aged at 1025°F for times up to 1000 hours exhibited the same level of hardening as the residual hardening just discussed.

Electron microscopy and scanning electron microscope (SEM) techniques were utilized to determine the propensity and nature of the precipitates encountered as well as to observe the morphology and distribution of the stable oxide dispersoid phase. The samples selected for the initial investigations were ODS 2062 and 2562 alloys in the annealed and the aged conditions: DR; aged 500 hours at 842°F; aged 500 hours at 1025°F. The samples were prepared by metallographic polishing with Linde B Al_2O_3 compound and followed by electropolishing. Preferential attack on the precipitated phase in the specimens aged at the 842°F (α') temperature prevented the study of those materials. The electron photomicrographs are shown in Figures 14 and 15. Alloy 2562 exhibited a grain boundary precipitate in the DR condition, while 2062 did not. Both alloys aged in the σ temperature range contained a grain boundary precipitate which occurred mainly in the regions which contained a relatively sparse oxide dispersion.

In the extrusion and secondary TMP of these materials the spherical preoxidized particles were elongated to long rod like shapes. The oxide film was fragmented and distributed along these oriented powder particles and boundaries gave rise to high density discontinuous oxide stringers between mating particles. During subsequent high temperature exposures the Fe9Y phase in the powder particles reacted with the Al_2O_3 particles and converted to a more complex oxide. This will be discussed in more detail in the Phase Identification Section. A significant percentage of these powder particles, for some unknown reason, remained clear of oxide. This might have been caused by very low concentrations of yttrium. It was these clear regions that were not converted to the desired coarse elongated grains. In addition, the precipitate was detected in the grain boundaries of the unconverted fine grains. The high density oxide regions seemed to retard both the undesirable retention of fine grains and age hardening.

A SEM investigation was performed on the 2562 + 4 v/o alloy exposed at 1025°F for 500 hours. Photomicrographs of the grain boundary precipitate phase and EDAX analysis are shown in Figures 16 and 17. Consistent with the modified Cr-Fe diagram presented in Figure 11, the precipitate was determined to be Sigma, a nearly equiatomic Fe-Cr composition. This finding does not, however, explain the retained hardness after the 1200° to 1400°F solution treatments.

To establish the effects of the aging treatments on the ODS FeCrAlY, tensile tests were conducted at RT, 500°, 1900° and 2100°F. Alloys 2062 and 2562 were evaluated in three material conditions: (1) DR (fully annealed); (2) DR and γ' aged; (3) DR and σ aged. The test results are presented in Table XIII and Figures 18 and 19. The RT tensile properties for two vane alloys, X-40 and MM509, are shown for comparison.

In the DR condition both 2062 and 2562 are stronger at RT than X-40 and MM509 and their ductility is at least as good. In the γ' aged condition there is a 45% increase in strength at RT for both 2062 and 2562 over the as-DR condition. The γ' aged Alloy 2562 at 500°F maintained a 41% increase in strength while Alloy 2062 fell to only 12% increase. Room temperature and 500°F testing of the σ aged Alloy 2062 showed very little difference in strength when compared to the initial DR condition. Alloy 2562, however, decreased about 7% at both temperatures. All FeCrAlY conditions seem to have at least marginally, ductility ranging from 1.4% elongation at RT in the γ' aged condition to 17.2% at 1900°F in the DR condition. The MM509 alloy is considered acceptable for vane applications at the 1.5 to 5.5% elongation level.

3.2 SURFACE STABILITY STUDIES

Although early work in the FeCrAlY family of alloys[8] indicated that Cr levels from 15 to 25 w/o yielded outstanding oxidation resistance, subsequent work by Stott[4] showed that at low Cr levels, the alloys were susceptible to break away oxidation. This phenomenon was found in the Ni, Co and Fe base MCrAlY alloys which were low in Cr content. Sporadic, rapid oxidation rates were observed in such alloys as a result of the formation of oxides other than the protective Al_2O_3 type. In cases where break away oxidation was observed in FeCrAl, the other scale formed was Fe_3O_4. An inner scale of complex Cr_2O_3, Fe_3O_4 and Al_2O_3 oxides resulted from rapid internal oxidation. The occurrences of break away oxidation found previously in some 15% Cr FeCrAlY powders was thought to be attributable to the very high surface to volume ratio found in these powders. The occurrences of this phenomenon in powder has raised concern with regard to application where surface contamination of Fe or Fe_3O_4 might initiate the phenomenon. An example of break away

oxidation on a piece of ODS 1562 .060" sheet material after an exposure of approximately 100 hours at 2400°F is shown in Figure 20. As a result of this concern, a test procedure was devised and candidate Alloys 1562, 2062 and 2562 were evaluated for resistance to break away oxidation which was intentionally initiated by surface contamination. Thus this test measured healing capacity of the alloy in the situation where localized inhomogenieties or surface contamination might initiate this unusual behavior. Specifically, the tests used specimens prepared from extruded rods of approximately 0.7" diameter which had a mild steel cladding of about 0.025" remaining on the FeCrAlY core. The cladded specimens were subjected to an exposure of 2400°F in air for 70 hours. The mild steel jacket initiated the Fe_3O_4 rapid oxidation, which progressed to the core/clad interface. In those alloys which were resistant to break away oxidation, the attack was halted at the interface by the formation of an internal Al_2O_3 scale. As can be seen from Table XIV and Figure 21, the two 1562 + 4 v/o oxide alloys suffered severe attack, fairly general in nature with metal loss of up to 0.150 inches. The 2062 + 4 v/o oxide alloy demonstrated good resistance with only isolated attack, approximately 0.070" penetration, and in good agreement with Stott's observation on the influence of Cr, the high Cr 2562 + 4 v/o alloy showed excellent resistance. Although 0.010" of metal was lost in Alloy 2562, it seems probable that at least part of that amount was attributable to loss in Cr due to interdiffusion between the mild steel cladding and the FeCrAlY core during TMP

The oxidation resistance of 2062 and 2562 alloys containing 4 v/o oxide was investigated at 2200°F and 2400°F in static air for exposure up to 500 hours. Som specimens were thermal cycled and weighed after each 100 hours while others were exposed uninterrupted. Conventional cast and wrought Alloys 1541 and 2541 were included for comparison. The ODS samples were prepared from rod rolled and directionally recrystallized materials, ground thru 600 grit silicon carbide papers to a shape approximately 0.55" dia. x 0.15" thick. The cast and wrought alloys were prepared from hot rolled plate in similar fashion.

The test results for the 2200°F oxidation exposures, in Table XV, show that weight changes in the ODS alloys were nearly equivalent to the conventional cast and wrought alloys. Also shown are the effects of thermal cycling on the oxide adherence. By visual inspection it was determined that there was more total spallation in the samples cycled each 100 hours than in the uninterrupted specimen which spalled in the final cool down.

The test results for oxidation at 2400°F are shown in Table XVI. After long times at this temperature, distinct differences in oxidation behavior between cast and wrought and ODS alloys were evident. The spalling resistance of the cast and wrought alloys was superior to that of the ODS alloys but this behavior was accompanied by a relatively deep intergranular oxide penetration which was absent in the ODS alloys. It is conceivable that in thin sections this intergranular penetration would degrade strength and ductility. Photographs of the oxidation specimens after testing are shown in Figure 22.

3.3 DIRECTIONAL RECRYSTALLIZATION STUDIES

The strength of oxide dispersion strengthened alloys is extremely sensitive to microstructural variations such as grain size, grain shape and texture. In an effort to gain further understanding and greater control of this effect, a directional recrystallization study was undertaken.

3.3.1 Equipment

The directional recrystallization (DR) technique requires that the recrystallization process be controlled by passing unrecrystallized material, with suitable starting microstructure, through a steep temperature gradient at a controlled rate. In order to achieve this experimentally, a heat source was positioned as close as possible to a heat sink, and the specimen was passed in a longitudinal direction from the heat sink into the heat source. Under the proper conditions, new grains were formed initially in the hot zone and grew in an opposite direction to the motion of the specimen. The first grains to form were relatively equiaxed but the steep temperature gradient suppressed nucleation of new grains and encouraged growth competition among existing grains. Those grains with the highest boundary mobility grew at the expense of those with less mobile boundaries. As the specimen traversed the gradient, the grain size increased to a maximum size which depended not only on the structure of the starting material, but also on several DR process parameters. These included steepness of the temperature gradient, rate of movement of the specimen, and orientation with respect to the working direction.

A schematic of the equipment used to produce this structure is shown in Figure 23, where the three principal parts of the apparatus may be seen quite distinctly. These include: (1) heat source - a flat induction coil: (2) heat sink - a water cooled Cu chill block: (3) specimen motion control - in this case a variable speed motor was used to drive a gear train which translated rotational motion to lateral motion. Lateral speeds achievable varied fromfrom 0.01 in/hour to 150 in./hour. Also shown in the schematic is an insulator which prevented arcing between the coil and the chill block. The specimen hot zone is shown as the shaded region immediately adjacent to the induction coil. The atmosphere surrounding the hot zone was either air or flowing argon (commercial grade) which was contained by a quartz tube. The 450 KCPS 10 KW power supply was controlled by an Ircon optical temperature monitor and control and an optical pyrometer was used for temperature measurements.

3.3.2 Material Preparation

Alloy 1562 + 4 v/o oxide was extruded at 1750°F using a 16:1 reduction ratio and this rectangular billet was subsequently isothermally forged at 1150°F/20% in the short transverse direction. When furnace recrystallized at 2400°F 2 hours, large elongated grains were formed. Pronounced anisotropy in grain boundary mobility was evidenced by the fact that the grains had typical dimensions of: l = 15mm, w = 4mm, t = 0.7mm. In order to investigate the DR response of this material, specimens were machined from unrecrystallized or "as-isothermal forged" material. Each of these specimens had different orientations in the original rectangular extrusion. Specimen A was prepared so that its longitudinal axis was parallel to the extrusion direction. Specimens of the B orientation were prepared with longitudinal axis in the long transverse direction, and specimens with the C orientation were taken in the short transverse direction. These orientations are shown in Figure 24.

3.3.3 Results

Directional recrystallization was performed on each of these materials as is shown in Figure 24 using the DR parameters listed in Table XVII. Typical grain dimensions, specimen sizes and corresponding DR parameters are also given in Table XVII. In the longitudinal and long transverse specimen, grain length was limited by specimen length, while in the short transverse specimen, grains did not traverse the full length of the

specimen. A sketch of the microstructures achieved in each of the three cases is also shown in Figure 24. As may be seen from the grain size results, grain boundary mobility was apparently anisotropic and in both the longitudinal and long transverse directions was considerably higher than in the short transverse.

Crystallographic orientation of these specimens has been completed and these results are shown in Figure 24. In specimen A, which was cut parallel to the extrusion direction and also DR processed in this same direction, the longitudinal axis was found to be parallel to the [110]. Laue back reflection photos of six different grains indicated that all were oriented within 2° of each other and the |110| in each was within 2° of the longitudinal axis.

Specimen B of Figure 24 was cut and DR processed in the long transverse direction. Laue back reflection photos of all three of the grains contained in the cross section indicated that the specimen axis was within approximately 3° of |111| in each. In the short transverse specimen C, only the two end grains were analyzed. The specimen axis was parallel to the [110] in one grain and to the |111| in the other. The as-extruded bar was analyzed for texture both by Laue transmission and on a diffractometer using Ni filtered Cu radiation. It was found that the alloy contained a |110| fiber texture and that approximately 50% of the material contained an orientation such that |110| was within 11° of the extrusion direction.

3.3.4 Stress-Rupture Evaluation

Stress-rupture properties were determined for the three DR conditions using small button head specimens, 0.187" diameter x 1.4" long, were step load tested at 2000°F in air. The longitudinal and long-transverse DR specimens had a gage section 0.1" in diameter x 0.50" in length. Because of limited material thickness (0.6") the short transverse specimens were modified to 0.1" diameter by 0.25" long. To facilitate the testing of these short sections they were made longer by brazing longitudinally DR 2062 alloy extensions onto each end. Joining was performed at 2550°F in vacuum using 0.005" thick Hastelloy X sheet as the braze alloy.

The stress-rupture test results are reported in Table XVIII. Subsequent to testing the specimens were ground longitudinally, macroetched and are shown photographically in Figures 25 and 26. The short transverse specimens C (No.'s 20-23) contained numerous grain boundaries oriented perpendicular to the stress axis. Specimen No. 23 recrystallized to a much larger grain size than did the others but still contained some short transverse boundaries running the full width of the gage. The braze joints are located just inside the threaded regions as can be seen in Figure 25.

The short transverse was found to be the weakest direction and consistently failed in short times at 2.0 ksi. In this direction both the transverse grain boundaries and the microstructural defects are aligned in the worst direction. As can be seen in the photographs, failure occurred in the grain boundaries which are the most detrimental defects. The two long-transverse specimens, B, contained no boundaries. Both specimens failed at the 5.0 ksi level during a step loading stress rupture test.

The specimen from the longitudinal direction (No. 4) was prepared from an isothermally forged rectangular bar that was upset at 1150°F to a 30% reduction in thickness. This specimen was recrystallized in a box furnace at 2400°F for 2 hours rather than DR. The specimen grew relatively small grains but these had a high aspect ratio. In the step-loaded rupture test at 2000°F specimen 4 failed after 1.5 hours at 6.5 ksi. Hence, even though

this specimen had a fine grain size and grain boundaries transverse to the stress axis, it was considerably stronger than the long transverse B specimen which had no boundaries transverse to the rupture stress axis. These results indicate that either the oxide stringers or the difference in crystallographic orientation which was [110] for the A-type specimen and [111] for the B type caused a decrease in strength.

As was anticipated, the type C short transverse specimen, with its numerous grain boundaries and oxide layers was the weakest material of the three.

3.4 STRESS-RUPTURE STUDIES

The largest contributors to strength are believed to be grain size and shape, dispersoid content and texture. Test results showing the effect of grain size are presented in Table XIX and Figure 27. Stress-rupture testing* was performed at 2000°F using step load techniques. The 2562 + 4 v/o oxide specimen (No. 14) in the unrecrystallized condition, initially loaded at 2.0 ksi failed after 6.4 hours at 2.5 ksi. A furnace recrystallized 1562 + 4 v/o oxide specimen (No. 5) with 0.1" long grains was initially loaded at 3.5 ksi and broke after 4.0 hours at 6.0 ksi. Another furnace recrystallized 1562 + 4 v/o oxide specimen (No. 4) with 0.2" long grains reached 6.5 ksi for 1.4 hours before failing. A third 1562 + 4 v/o oxide specimen was fabricated from a three-inch long directionally recrystallized rod with the grains running the full length. This test specimen (No. 2) contained no transverse grain boundaries and was initially tested at 6.5 ksi for 500.6 hours. As the data indicates there is a very dramatic improvement in strength with increasing grain size.

A stress-rupture property study was conducted on ODS FeCrAlY alloys with the higher chromium content: 2062 and 2562, both containing 4 v/o oxide. The extrusion, TMP and DR of these alloys were performed as described in the Thermal Stability Studies Section of this report. The alloy chemistries are shown in Table VIII. The stress-rupture test results are presented in Table XX and Figure 28.

The 2562 + 4 v/o oxide alloy demonstrated strengths for short times (112 hours or less) of 7.5 ksi at 1900°F, 7.0 ksi at 2000°F and 6.5 ksi at 2100°F. Most of the 2062 + 4 v/o oxide stress-rupture specimens are still running, making it difficult to assess the strength, but based on the two failed specimens it appears it will be somewhat lower than the 2562 + 4 v/o oxide alloy. This difference in strength was not anticipated and is not considered to be attributable to the variation in chrome content. Previous testing of the 1562 + 4 v/o oxide alloy exhibited strengths as high as 8.0 ksi. Possibly this difference is reflected in the vacuum fusion results shown in Table VIII. The 2562 + 4 v/o oxide alloy analyzed at 1.1881% oxygen and the 2062 + 4 v/o oxide alloy at 0.9077% oxygen. This is a 30% difference in oxide content and might explain the variation in strength.

*Button head specimens 0.178" in diameter x 1.4" long with a 0.1" diameter x 0.5" long gage section were used throughout this program. Thermocouples were wired to the gage for temperature control and stress was applied using direct loading techniques.

To determine the effects of high temperature long time exposures on the strength properties of these alloys, specimens were heated for 100 hours at 2200°F and 2400°F in air prior to stress-rupture testing. The test results are shown in Table XXI. The data is plotted in comparison with the as-directionally recrystallized alloys and shown in Figure 29. With the exception of the 2562 + 4 v/o oxide alloy, specimen heated at 2200°F for 100 hours both alloys suffered losses in strength at a constant Larsen Miller parameter. The 2562 + 4 v/o oxide alloy heat treated at 2400°F for 100 hours showed a decrease of about 20%. The 2062 + 4 v/o oxide alloy specimen heat treated at 2200°F and 2400°F for 100 hours showed losses of at least 30 and 25 respectively.

The loss in the strength associated with the high temperature exposures pointed suspiciously at DR temperatures. DR is performed in a 2450-2550°F temperature range. If the heat treatments at 2200° and 2400°F for 100 hours could degrade strength maybe the higher temperature 2550°F DR temperature at short times could be detrimental. Selected specimens were prepared using DR temperatures ranging from 2450°F down to 2200°F and tested in stress-rupture. The results are shown in Table XXII and Figure 30. As can be seen in Figure 30 where the data is compared with the material processed at the higher DR temperatures (2450-2550°F) there is no indication that lower DR temperatures were beneficial. In fact, the 2062 + 4 v/o oxide alloy recrystallized at 2250°F showed a loss of strength.

3.5 OPTIMIZATION OF OXIDE CONTENT

An ODS 2562 + 6 v/o oxide alloy was prepared for evaluation. Atomized powders from Table I were pre-oxidized to 1.43 w/o oxygen at 1225°F for 10.5 hours in shallow trays at a 0.2" powder depth. The pre-oxidized powder was canned in a 3" diameter mild steel extrusion capsule and extruded at 1750°F and a 16 to 1 reduction in area to a 0.75" diameter rod. The extruded rod was sound and of good appearance. Recrystallization response of the 6 v/o oxide alloy was determined by inserting a small section into a furnace at 2400°F for 2 hours. Macro etching revealed no large grains had formed.

Rod rolling a piece of the extruded rod at 1500°F to a 20% reduction in area and heat treating at 2400°F for 2 hours produced the desired large grain structure. The remaining 6" length of the rod rolled material was directionally recrystallized for evaluation. Stress-rupture properties were measured at 2000°F using three miniature button head specimens utilizing the step load technique. The test results are reported in Table XXIII. All three specimens were initially loaded at 6.5 ksi and increased by 0.5 ksi about every 24 hours. Specimen No. 17-1 failed at the 6.5 ksi level after 16.1 hours. The remaining two specimens No.'s 17-2 and 17-3 both reached 9.0 ksi before failing. One lasted 1.3 hours and the other 0.3 hours.

As shown in Figure 31 the 9.0 ksi strength of the 2562 + 6 v/o oxide alloy specimens which were rod rolled to a 20% reduction represents a 20% increase in strength when compared to the average strength of the 2562 + 4 v/o oxide alloy also rod rolled to a 20% reduction. This strength level is 90 times that of the conventional cast and wrought FeCrAlY. Also reported in the Figure 31 are the strengths of TD NiCr sheet and the density corrected curve for the ODS 2562 + 6 v/o oxide alloy. This correction is obtained using a stress multiplying factor derived by dividing the density of the TD NiCr by the density of ODS FeCrAlY. With the density allowance the ODS 2562 + 6 v/o oxide alloy is stronger than TD NiCr sheet.

3.6 PHASE IDENTIFICATION AND MORPHOLOGY

Oxide dispersion strengthened FeCrAlY alloys prepared analogous to the SAP approach contain a nonuniform spatial array of oxide with a wide range of particle size. Alloys containing 4 v/o oxide have particles nearly spherical in shape and range in size from < 250 Å to > 1 micron. The average particle size and interparticle spacing is 0.19 and 2.49 microns respectively.

Identification of the oxide phases were established for both the as-extruded and heat treated conditions. The oxide phases were extracted electrolytically in a 10% solution of HCL-CH_3ON. Identification was made by x-ray diffraction. An 2062 + 4 v/o oxide alloy extruded at 1950°F to a 16:1 reduction ratio was determined to contain about 85% Y_2O_3, 10% $YAlO_3$ and 5% Al_2O_3. Three alloys (1562 + 4 v/o, 2062 + 4 v/o, 2562 + 4 v/o oxide) heat treated at 2400°F for 100 hours contained about 60% $Al_2O_3 \cdot 3Y_2O_3$, 30% $5Al_2O_3 \cdot 3Y_2O_3$, and 10% $YAlO_3$. The results were independent of alloy composition.

Scanning Electron Microscope (SEM) analysis was performed on the 2562 + 4 v/o oxide alloy that was thermally exposed at 2400°F for 100 hours. The photographs showing the microstructure and the Energy Dispersion Analysis X-Ray (EDAX) results are presented in Figure 32. The SEM/EDAX results corroborates the results obtained using the extraction technique. The oxide particles are yttrium • aluminum.

4. DISCUSSION

Two major problems previously encountered in the development of ODS FeCrAlY alloy have been overcome: surface stability and powder pre-oxidation. ODS 1562 + 4 v/o oxide alloy was determined to suffer "breakaway" oxidation when exposed in wrought form at very high temperatures or in powder form at relatively low temperatures as shown in Figures 20 and 3 respectively. Increasing the chromium content to 20% and 25% virtually eliminated "breakaway" as evidenced in Figures 4, 5, 21 and 22.

Uniform, controllable pre-oxidation of powder has been achieved. In the past, powder pre-oxidation was attempted in a common box furnace with a static air flow, using either trays containing the powder or in sealed retorts with a dynamic flow of pure oxygen gas. In the interest of quantity the powder depths ranged from 0.6" to 3.5". When air was the oxidizing gas nitrogen contamination occurred at powder depths of approximately 0.5" and below. Studies investigating the oxidation of the -325 mesh powder as a function of powder depth determined the safe working depth to be about 0.25 inches.

Several new powder pre-oxidation techniques were established. Good uniformity and reproducibility was obtained in the static tray approach where powder depths were limited to 0.25 inches or less. For the preparation of large quantities the rotary kiln and moving tray processes were investigated and endorsed. In the rotary kiln the powder is tumbled during pre-oxidation, continuously exposing fresh material to the environment. In the moving tray approach the powder is spread in shallow trays and traversed through the furnace on a conveyor system. These techniques placed all the powder particles in easy access to the oxidizing gas.

Thermal stability of the ODS FeCrAlY was investigated in the intermediate temperature range. In the Fe-Cr system as shown in Figure 11, two age hardening precipitates are encountered: a nearly equi-atomic FeCr phase (σ) which forms at temperatures below 1500°F and a chromium rich ferrite phase (α') that forms below 970°F. Experiments were conducted to establish the propensity of the precipitates and their effects on properties. The aging response is reported in Tables No. IX and X and the effects on tensile properties are reported in Table XIII. The materials aged in the σ region showed only slight increases in hardness and effect on properties. The materials aged in the α' region increased considerably in hardness ranging from 38% for the 15%Cr level to 80% for the 25 chrome level and showed very significant increases in tensile strength at RT. At the 500°F test temperature the 25%Cr alloy maintained most of its increased strength. The increased strength of the 20% Cr alloy fell sharply. Ductility of these alloys at RT dropped from 6% to 3% in the 20%Cr and to 2% in the 25%Cr alloy.

Stress-rupture properties were determined for the ODS 2062 + 4 v/o oxide and ODS 2562 + 4 v/o oxide alloys in a 20% rod rolled and DR condition and the results are given in Table XX. The short time strengths at 2000°F for the 25%Cr alloy was determined to be 7.5 ksi. The 20%Cr alloy showed strengths somewhat lower than the 25%Cr alloy. This lower strength was thought to be due to a lower volume fraction of oxides in the 20% chromium alloy.

An ODS 2562 + 6 v/o oxide alloy was prepared and tested similar to the ODS 2562 + 4 v/o oxide alloy. Short time strength was found to be at the 9.0 ksi level and represents a 20% increase in strength.

5. CONCLUSIONS

1. Powder pre-oxidation of the ODS FeCrAlY alloys is much improved with increased chromium content. "Breakaway" oxidation has been eliminated in the 20% and 25% chromium bearing alloys, both as powder and bulk alloy.

2. FeCrAlY -325 mesh powders can be uniformly pre-oxidized in air without nitrogen contamination by limiting the powder depth to 0.25" or by tumbling the powder during the exposure.

3. Stress-rupture property studies were conducted on the 2062 + 4 v/o oxide and 2562 + 4 v/o oxide alloys at 1900, 2000 and 2100°F. The 2562 + 4 v/o oxide alloy in the rod rolled and DR condition possess short time strengths of 7.5 ksi at 2000°F. With allowance for the difference in densities, the 2562 + 4 v/o oxide alloy is as strong as TD NiCr sheet.

4. The effects of 2200°F and 2400°F exposure for 100 hours in air were determined on the stress-rupture strengths of the 2062 + 4 v/o and 2562 + 4 v/o oxide alloys. Alloy 2562 + 4 v/o oxide was stable to exposure at 2200°F, but after exposure at 2400°F showed a decrease of about 20% in rupture strength at 2000°F. The 2062 + 4 v/o oxide alloy specimen heat treated at 2200°F and 2400°F showed losses of 30% and 25% in 2000°F rupture strength.

5. The effects of DR temperatures (2200, 2250, 2450°F) on 2000°F stress-rupture properties were investigated. There was no indication that lower DR temperatures were beneficial.

6. A 2562 + 6 v/o oxide alloy was prepared and evaluated in stress-rupture at 2000°F. The rod rolled and DR alloy demonstrated short time strengths of 9.0 ksi. With the allowance for the difference in density, the 2562 + 6 v/o oxide alloy is stronger than TD NiCr sheet.

7. Aging studies were conducted on ODS 1562, 2062 and 2562 containing 4 v/o oxide at 842°F (α') and 1025°F (σ). Exposures at 842°F for 1000 hours showed the propensity of precipitation hardening to increase with increasing chromium content: the 1562 alloy increased in hardness by 39%; the 2062 by 70%; and the 2562 alloy by 80%. Hardness increases at 1025°F were much lower; the 1562 alloy increased only 4%; 2062 9%; and the 2562 alloy 17%.

8. The 2062 + 4 v/o and 2562 + 4 v/o oxide alloys aged at 842°F for 500 hours were tested in tension at RT and 500°F to determine the effects on properties. The 2062 + 4 v/o and 2562 + 4 v/o alloys aged at 842°F (α') showed strength increases at RT of 45% (190 and 203 ksi). At 500°F the 2062 + 4 v/o oxide alloy fell to an increase of only 13% while the 2562 + 4 v/o oxide alloy maintained 41% increase.

9. The 2062 + 4 v/o and 2562 + 4 v/o oxide alloys aged at 1025°F for 500 hours were tested in tension at RT and 500°F to determine the effects on properties. The 2062 + 4 v/o oxide alloy showed very little difference in properties at either temperature when compared to the unaged DR condition. The 2562 + 4 v/o oxide alloy suffered a 7% loss in strength at both temperatures.

10. Electron microscopy and SEM analysis techniques were utilized to locate and identify the precipitate which formed at the 1025°F aging exposure and was determined to be Sigma phase.

11. Exposure at 1200°F for 10 minutes after aging at 842°F restores properties essentially to unaged levels.

6. REFERENCES

1. R. E. Allen, Final Report Naval Air Systems Command Contract No. N00019-69-C-0149, January, 1970.

2. R. E. Allen, Final Report Naval Air Systems Command Contract No. N00019-70-0232, January, 1971.

3. R. E. Allen, and R. J. Perkins, Final Report Naval Air Systems Command Contract No. N00019-71-0100. April. 1972.

4. F. H. Stott, G. C. Wood and M. G. Hobby, Oxidation of Metals. Vol. 3. No. 2, 1971.

5. R. O. Williams, Trans. TMS-AIME 1958. Vol. 212. p. 497.

6. C. S. Wukusick, AEG Contract AT (40-1)-2847. Report No. GEMP-414, June, 1966.

7. P. J. Grobner, Trans. TMS-AIME 1973. Vol. 4. No. 1. p. 251.

8. C. S. Wukusick and J. F. Collins, Materials Research and Standards, Vol. 4, No. 12, 1964, p. 637.

ACKNOWLEDGEMENTS

Appreciation is extended to Dr. C. A. Bruch who has provided excellent guidance throughout the program and to G. L. McCabe who assisted in various phases of the experimental work.

TABLE I

CHEMICAL ANALYSIS OF AS-RECEIVED
ARGON ATOMIZED FeCrAlY POWDERS

Element	Content, w/o		
	Alloy 1562	Alloy 2062	Alloy 2562
Fe	Balance	Balance	Balance
Cr	16.48	20.21	25.08
Al	5.89	5.97	5.89
Y	1.9	2.08	2.09
C	.009	.010	.010
Si	.066	<.10	.096
P	.002	.003	.003
O	.072	.074	.074
N	.0081	.007	.009
H	.0037	.005	.005

TABLE 11

WEIGHT GAIN OF ALLOY 1562 -325 MESH POWDER
DURING AIR OXIDATION IN PORCELAIN CRUCIBLES

Speciman Number	Temperature °F	Powder Depth Inches	% Weight Gain			Comments
			2 hrs	6 hrs	22 hrs	
6	1100	.37	.84	1.01	1.19	Uniform color
7	1100	.37	.84	.96	1.23	Uniform color
8	1100	.37	.84	.96	1.22	Uniform color
9	1100	.37	.83	.93	1.23	Uniform color
10	1100	.37	.84	.94	1.23	Uniform color
1	1150	.37	.95	1.09	1.31	Uniform color
2	1150	.37	.95	1.10	1.31	Uniform color
3	1150	.37	.94	1.08	1.30	Uniform color
5	1150	.37	.94	1.08	1.30	Uniform color

TABLE III

WEIGHT GAIN OF ALLOY 2062 -325 MESH POWDER DURING AIR OXIDATION IN PORCELAIN CRUCIBLES

Specimen Number	Temperature °F	Powder Depth Inches	% Weight Gain			Comments
			2 hrs	4 hrs	20 hrs	
29	1200	.25	.93	1.04	1.43	Uniform color
30	1200	.25	.90	1.02	1.40	Uniform color
25	1200	.4	.91	1.02	1.40	Uniform color
26	1200	.4	.92	1.03	1.42	Uniform color
27	1200	.4	.91	1.03	1.41	Uniform color
28	1200	.4	.92	1.04	1.43	Uniform color
23	1300	.25	1.17	1.35	1.79	Uniform color
24	1300	.25	1.18	1.36	1.82	Uniform color
19	1300	.4	1.17	----	----	Uniform color
20	1300	.4	1.18	1.35	1.79	Uniform color
21	1300	.4	1.20	1.36	1.81	Uniform color
22	1300	.4	1.17	1.35	1.76	Uniform color
13	1400	.1	----	----	----	Uniform color
16	1400	.1	1.59	1.80	2.43	Uniform color
12	1400	.25	1.63	1.83	2.47	Uniform color
17	1400	.25	1.63	1.82	----	Uniform color
11	1400	.5	1.66	1.85	2.52	Non-uniform color - top .4" med. blue - bottom .1" light blue
14	1400	.5	1.66	1.85	2.53	
15	1400	.5	1.65	1.85	2.52	
18	1400	.5	1.64	1.83	----	

TABLE IV

WEIGHT GAIN OF ALLOY 2562 -325 MESH POWDER DURING AIR OXIDATION IN PORCELAIN CRUCIBLES

Specimen Number	Temperature °F	Powder Depth Inches	% Weight Gain			Comments
			2.2 hrs	4.2 hrs	20.2 hrs	
39	1200	.1	1.02	1.14	1.46	Uniform color
43	1200	.1	1.05	1.11	1.44	Uniform color
46	1200	.3	1.02	1.10	1.42	Uniform color
40	1200	.4	1.02	1.11	----	Uniform color
44	1200	.4	1.04	1.13	1.45	Uniform color
41	1200	.6	1.02	1.11	1.40	Top .5" med. blue
45	1200	.6	1.11	1.10	1.40	Bottom .1" light brown
42	1200	.3	1.01 (a)	----	----	

(a) Vacuum fusion analysis - 2.2 hrs - T
Top = .975% O_2, .0067% N_2
Bottom = 1.037% O_2, .0617% N_2

TABLE V

FeCrAlY POWDER PREOXIDATION RUNS

Powder	% Oxygen, As-Atomized	Type Preoxidation	Powder Depth, in.	Temp. °F	Time Hrs.	Atmos.	Weight Gain %	% Oxygen (Vac. Fusion)	Color Uniformity
1562	.072	-	-	-	-	-	-	-	-
1562	.072	Static	.30	1100	6	Air	1.0	1.0	Excellent
1562	.072	Static	.25	1100	6	Air	1.0	1.0	Excellent
1562	.072	Static	.25	1100	6	Air	1.0	-	Excellent
2062	.074	-	-	-	-	-	-	-	-
2062	.074	Static	.40	1175	4	Air	1.0	1.1	Layer effect - bottom layer removed.
2062	.074	Static	.25	1175	4	Air	1.0	0.9	Excellent
2062	.074	Static	.25	1175	4	Air	1.1	-	Excellent
2032	.074	Conveyor	.25	1175	4	Air	1.0	-	Excellent
2562	.074	-	-	-	-	-	-	-	-
2562	.074	Static	.40	1175	2	Air	1.0	-	Layer effect - bottom layer removed.
2562	.074	Static	.25	1175	2	Air	1.0	1.2	Excellent
2562	.074	Static	.25	1175	2	Air	1.0	-	Excellent

TABLE VI

CHEMICAL ANALYSIS OF 1562 BEFORE AND AFTER ROTARY PREOXIDATION

Element	As-Received	Preoxidized
Fe	Bal.	-
Cr	16.48	-
Al	5.89	-
Y	1.90	-
C	.009	-
O	.072	0.9
N	.008	.0001
H	.004	.0015
Ag	T[1]	T
Cu	T	T
Mg	T	T
Mn	T	T
Ni	T	T
Si	.066	T

[1] T = Trace (< 1%)

TABLE VII

CHEMICAL ANALYSIS OF 2062 ALLOY BEFORE AND AFTER PREOXIDATION USING THE MOVING TRAY APPROACH

Element	As-Received	Preoxidation
Fe	Bal.	-
Cr	19.95	-
Al	5.74	-
Y	1.74	-
C	0.0140	0.0002
O	0.0739	1.0788
N	0.0037	0.0047
H	0.0023	0.0017
Ag	0.0135	T
Cu	T[1]	T
Mg	T	T
Mn	T	T
Ni	T	T
Si	T	T

[1]T = Trace (< 1%)

TABLE VIII

CHEMISTRIES OF STARTING MATERIALS FOR AGING STUDIES

	ODS Alloys			Cast and Wrought	
	1562	2062	2562	2541	1541
Fe	Bal.	Bal.	Bal.	Bal.	Not available
Cr	16.59	20.21	25.08	24.55	
Al	5.70	5.97	5.89	3.83	
Y	1.98	2.08	2.09	1.23	
C	0.010	-	-	0.04	
Si	0.066	< 0.10	0.096	0.15	
P	0.002	0.003	0.003	-	
O	0.9819	0.9077	1.1881	0.001	
N	0.0028	0.0043	0.0040	0.001	
Ag	T[a]	0.014	0.001	-	
Mg	T	T	T	-	
Mn	T	T	T	-	
Ni	T	T	T	-	

(a) Semi-quantitative spectrographic analysis, T = 0 - 1%

TABLE IX

HARDNESS OF FeCrAlY ALLOYS AS A FUNCTION OF AGING TIME AT 842°F

Material	Condition	Rc Hardness at Various Exposure Times (Hrs.) 0	24	48	108	273	500	1000	Total R_c Hardness Increase
1562 (Ext. 6)	As-ext.	26	28	28	29	32	34	36	10
2062 (Ext. 13)	DR(1)	23	29	30	32	37	37	39	16
	RR(2)	32	35	36	38	40	42	43	11
2562 (Ext. 14)	DR(1)	24	33	34	35	40	42	43	19
	RR(2)	33	39	40	41	45	45	47	14
1541 Conv.	Plate	8	10	10	11	16	20	24	16
2541 Conv.	Plate	9	20	20	25	28	31	32	23

(1) DR - Directionally Recrystallized

(2) RR - As Rod-Rolled

TABLE X

HARDNESS OF FeCrAlY ALLOYS AS A FUNCTION OF AGING TIME AT 1025°F

		Rc Hardness at Various Exposure Times (Hrs.)							
Material	Condition	0	24	48	108	273	500	1000	Total R_C Hardness Increase
1562 (Ext. 6)	As-ext.	26	27	27	27	28	27	27	1
2062 (Ext. 13)	DR[1]	23	26	25	26	26	26	25	2
	RR[a]	32	34	33	33	34	34	33	1
2562 (Ext. 14)	DR	24	29	28	28	29	29	28	4
	RR	33	35	38	35	35	35	35	2
1541 Conv.	Plate	8	8	7	7	9	8	8	0
2541 Conv.	Plate	9	14	14	12	14	14	11	5

[1] Directionally Recrystallized

[a] As-Rod Rolled

TABLE XI

ODS FeCrAlY SOLUTION ANNEALING STUDY

Material	Material Condition	Original Hardness R_c	500 Hour Aging Temperature	Hardness, Rc	Temp., °F	Time, Hrs.	Solutioned Hardness R_c
1562 + 4 v/o	As-ext.	26	842F	33	1200	0.1	27
						0.3	27
						1.0	28
					1300	1.0	27
					1300	2.0	27
			842F + 1200F/1 hr.	28	1400	0.2	27
						1.0	27
						17.0	27
2062 + 4 v/o	DR	23	842F	37	1200	0.1	25
						0.3	26
						1.0	26
					1300	1.0	25
					1300	2.0	26
			842F + 1200F/1 hr.	26	1400	0.2	25
						1.0	25
						17.0	26
			842F	37	2000	2.0	23
2562 + 4 v/o	DR	24		42	1200	0.1	28
						0.3	28
						1.0	28
					1300	1.0	28
						2.0	28
			842F + 1200F/1 hr.	28	1400	0.2	27
						1.0	27
						17.0	28
			842F	42	2000	20	20

TABLE XII

ODS FeCrAlY SOLUTION ANNEALING STUDY

Material	Condition	Original Hardness Rc	500 Hour Aging Treatment	Aged Hardness, Rc	Solution Temp., °F	Time, Hrs.	Solutioned Hardness, Rc
1562 + 4 v/o	As-ext.	26	1025F	26	1200	0.1	27
"	"	"	"	"	"	0.3	26
"	"	"	"	"	"	1.0	27
"	"	"	"	"	1300	1.0	28
"	"	"	"	"	"	2.0	27
"	"	"	1025F + 1200F/1 hr.	27	1400	0.2	"
"	"	"	"	"	"	1.0	"
"	"	"	"	"	"	17.0	"
2062 + 4 v/o	DR	23	1025F	25	1200	0.1	25
"	"	"	"	"	"	0.3	27
"	"	"	"	"	"	1.0	26
"	"	"	"	"	1300	1.0	25
"	"	"	"	"	"	2.0	26
"	"	"	1025 + 1200F/1 hr.	26	1400	0.2	27
"	"	"	"	"	"	1.0	26
"	"	"	"	"	"	17.0	"
"	"	"	"	"	2000	2.0	23
2562 + 4 v/o	"	24	1025	27	1200	0.1	27
"	"	"	"	"	"	0.3	28
"	"	"	"	"	"	1.0	"
"	"	"	"	"	1300	1.0	"
"	"	"	"	"	"	2.0	"
"	"	"	1025 + 1200F/1 hr.	28	1400	0.2	"
"	"	"	"	"	"	1.0	"
"	"	"	"	"	"	17.0	29
"	"	"	"	29	2000	20	25

TABLE XIII

TENSILE TEST RESULTS OF DIRECTIONALLY RECRYSTALLIZED ODS FeCrAlY ALLOYS IN BOTH AGED AND AS-DIRECTIONALLY RECRYSTALLIZED CONDITIONS

Material	Condition	Hardness, R_c	Test Temp., °F	0.2% Yld. Str., ksi	Ultimate Str., ksi	% Elong.	% R of A
2062 + 4 v/o	DR[a]	23	RT	107.0	132.0	8.3	18.1
	Aged 1025°F[b]	26	RT	102.7	133.9	10.4	20.8
	Aged 842°F[c]	37	RT	189.0	190.0	3.0	4.0
	DR	23	500	86.5	128.0	6.1	6.8
	Aged 1025°F	26	500	82.1	125.0	7.8	5.8
	Aged 842°F	37	500	137.0	144.0	1.4	1.0
	DR	23	1900	11.0	11.1	13.0	32.3
	DR	23	2100	8.3	8.8	7.2	7.8
2562 + 4 v/o	DR	24	RT	110.0	140.0	7.7	14.4
	Aged 1025°F	29	RT	-	130.6	8.0	13.6
	Aged 842°F	42	RT	201.0	203.0	2.2	4.0
	DR	24	500	87.3	131.0	6.5	11.6
	Aged 1025°F	29	500	81.1	122.0	5.5	4.9
	Aged 842°F	42	500	184.0	185.0	1.9	3.0
	DR	24	1900	12.2	12.9	17.4	50.5
	DR	24	2100	9.4	9.7	9.2	60.0
X-40	As Cast & HT	-	RT	75.0	115.0	10/3.5[d]	-
MM509	As Cast & HT	-	RT	80.0	110.0	3.5/1.5	4.0/1.5

[a] Directionally recrystallized 2450-2550°F

[b] Aged in Sigma region for 500 hours

[c] Aged in Alpha region for 500 hours

[d] Average/three standard deviations under average

TABLE XIV

RESISTANCE OF CANDIDATE ALLOYS TO BREAKAWAY OXIDATION[a]

Extrusion No.	Alloy	Minimum Core Dia., in.	Maximum Penetration	Healing Quality
8	(rotary) 1562	.670	~ 150 mils	Poor
10	1562	.670	~ 150 mils	Poor
9	2062	.63	~ 70 mils	Good, isolated attack
11	2562	.65	~ 10 mils	Excellent

(a) Specimen exposed to static air at 2400F/70 hr. - specimen were 1/2" long rods which had a 25 mil mild steel clad on the outer diameter.

TABLE XV

OXIDATION RESISTANCE OF SELECTED FeCrAlY ALLOYS AS A FUNCTION OF TIME AT 2200F IN STATIC AIR

Specimen No.	Alloy	Wt. Increase (mg/cm^2) vs Time (Hrs.) 112	200	300	400	500	Oxide Spall Rating
1	2062 + 4 v/o oxide	1.4	1.9	1.9	1.3	0.6	Moderate
2	"		Uninterrupted			2.4	Very Slight
7	2562 + 4 v/o oxide	1.4	1.7	1.3	0.7	0	Moderate
8	"		Uninterrupted			2.7	Moderate
13	1541 Conv. (a)	2.3	2.9	3.2	3.4	3.4	Very Slight
15	2541 Conv.	1.9	2.4	2.6	3.0	3.0	Moderate

(a) Cast and Wrought

TABLE XVI

OXIDATION RESISTANCE OF SELECTED FeCrAlY ALLOYS AS A FUNCTION OF TIME AT 2400F IN STATIC AIR

Specimen No.	Alloy	Wt. Change (mg/cm^2) vs Time (Hrs.) 100	200	300	400	500	Oxide Spall Rating
3	2062 + 4 v/o oxide	3.0	1.3	-1.3	-3.8	-7.3	Gross
4	"	← Uninterrupted →				-0.8	
9	2562 + 4 v/o oxide	1.8	-0.9	-4.6	-7.7	-11.1	
10	"	← Uninterrupted →				-1.5	
14	1541 Conv.[a]	4.7	5.8	6.6	7.3	7.9	
16	2562 Conv.[a]	4.6	5.3	5.3	5.4	4.8	

[a] Cast and wrought

TABLE XVII

DR PARAMETERS USED FOR SPECIMENS A, B, AND C OF FIGURE 4

Spec. Configuration	A	B	C
Shape	Rectangular	Round	Round
Dimensions (mm)	57 X 20 X 14	38 X 5.5 dia.	15 x 5.5 dia.
Orientation			
DR Rate (in./hr.)	1	1	1
Temp. (°F)	2400	2500	2500
Grad. (approx.) °F/in.	1000	3500	3500
Heat Source	Induct.	Induct.	Induct.
Heat Sink	Ambient Air	H_2O Cooled Cu Chill	H_2O Cooled Cu Chill
Resulting Grain Size			
Length (mm)	57	50	2.0
Width (mm)	11	5.5	5.0
Thickness (mm)	.7	2.0	5.5

TABLE XVIII

STRESS-RUPTURE STRENGTHS AT 2000°F OF ALLOY 1562 + 4 v/o OXIDE AFTER DIRECTIONAL RECRYSTALLIZATION IN VARIOUS DIRECTIONS

Spec. No.	DR Direction*	Stress, ksi	Rupture Life, Hrs.	% Elong.	% R of A
20	C	2.0	2.9	8.0	2.0
21	C	2.0	1.5	4.0	2.0
22	C	2.0	2.0	9.5	3.0
23	C	2.0	23.5	3.8	7.0
24	B	4.0	25.3	Step load to	
		4.5	24.0	Step load to	
		5.0	0.6	--(a)	5.7
25	B	4.5	24.3	Step load to	
		5.0	3.2	10.0	4.8
4	A (furnace recrystallized)	3.5	25.2	Step load to	
		4.0	25.4	"	
		4.5	24.3	"	
		5.0	25.3	"	
		5.5	24.3	"	
		6.0	24.0	"	
		6.5	1.5	--(a)	--(a)

(a) Could not piece broken sections together after fracture to make measurements.

*A = Longitudinal; B = Long transverse; C = Short transverse

TABLE XIX

EFFECT OF GRAIN SIZE ON STRESS RUPTURE STRENGTH OF ODS FeCrAlY at 2000°F

Spec. No.	Alloy	Material Condition	Grain Size Length x in.	Stress, Ksi	Time, Hrs.	Elong.,%	R.A., %
14	2562	Un Rx[a]	-	2.0	42.3		
				2.5	6.4	10.4	2.6
5	1562	Furn Rx[b]	0.1"	3.5	25.1		
				4.0	23.7		
				4.5	41.0		
				5.0	24.0		
				5.5	24.0		
				6.0	4.0		
4	1562	Furn Rx	0.2"	3.5	25.2		
				4.0	25.4		
				4.5	24.3		
				5.0	25.3		
				5.5	24.3		
				6.0	24.0		
				6.5	1.5		
2	1562	DR[c]	0.5"[d]	6.5	500.6		
				7.0	27.0		
				7.5	19.0		
				8.0	0.6		

[a] Unrecrystallized, As-Rod-Rolled

[b] Furnace Recrystallized at 2400°F for 2 hours

[c] Directionally Recrystallized

[d] Material directionally recrystallized to several inches in length, but the specimen gage section is only 0.5" long.

TABLE XX

STRESS RUPTURE STRENGTHS OF DIRECTIONALLY RECRYSTALLIZED ODS FeCrAl ALLOYS

Alloy	Test. Temp. °F	Stress, Ksi	Rupture Life, Hrs.	% Elong.	% R of A	
2062 + 4 v/o	1900	5.6	340	Still Running		
2062 + 4 v/o	1900	6.1	320	Still Running		
2062 + 4 v/o	2000	4.0	46.9[a]			
2062 + 4 v/o	2000	4.5	25.8[a]			
2062 + 4 v/o	2000	5.0	25.4[a]			
2062 + 4 v/o	2000	5.5	5.8	1.9	2.1	
2062 + 4 v/o	2000	5.0	674	1.0	Nil	Terminated no rupture
2062 + 4 v/o	2100	4.5	626	Still Running		
2062 + 4 v/o	2100	5.1	22.5	16.0	23.6	
2562 + 4 v/o	1900	7.0	410	Still Running		
2562 + 4 v/o	1900	7.5	112.4	6.0	22.7	
2562 + 4 v/o	2000	4.0	24.6[a]			
2562 + 4 v/o	2000	4.5	24.9[a]			
2562 + 4 v/o	2000	5.0	23.9[a]			
2562 + 4 v/o	2000	5.5	114.2[a]			
2562 + 4 v/o	2000	6.0	28.2[a]			
2562 + 4 v/o	2000	6.5	25.3[a]			
2562 + 4 v/o	2000	7.0	10.1	11.8	23.0	
2562 + 4 v/o	2000	6.5	62.0	7.7	30.3	
2562 + 4 v/o	2000	6.5	190.9	11.8	6.1	
2562 + 4 v/o	2100	5.8	46.7	10.2	35.0	
2562 + 4 v/o	2100	6.5	6.8	16.0	34.3	

[a] Stress increased by 0.5 Ksi

TABLE XXI

STRESS RUPTURE STRENGTHS AT 2000°F OF DIRECTIONAL RECRYSTALLIZED ODS FeCrAlY ALLOYS SUBSEQUENT TO LONG TIME HIGH TEMPERATURE EXPOSURES IN AIR

Alloy	Heat Treatment	Stress, Ksi	Rupture Life, Hrs.	% Elong.	% R of A
2062	2200°F-100 hrs.	5.0	1.6	3.8	13.5
2062	2400°F-100 hrs.	5.0	5.5	2.9	5.9
2562	2200°F-100 hrs.	6.5	57.7	2.4	-
2562	2400°F-100 hrs.	6.5	0.8	-	7.8

TABLE XXII

STRESS RUPTURE STRENGTHS AT 2000°F OF ODS FeCrAlY ALLOYS DIRECTIONALLY RECRYSTALLIZED AT VARIOUS TEMPERATURE

Alloy	DR Temp., °F	Stress, Ksi	Rupture Life, Hrs.	% Elong	% R of A
2062	2250	5.5	24		
		6.0	1.4	-	-
2062	2250	5.5	51.4		
		6.0	17.4	8.6	30.8
2562	2200	7.0	24.0		
		7.5	5.5	-	-
2562	2450	7.0	24.0		
		7.5	1.5	3.9	31.5

TABLE XXIII

STRESS RUPTURE RESULTS OF ODS 2562 + 6 v/o OXIDE AND 1562 + 4 v/o OXIDE ALLOYS TESTED AT 2000°F

Spec. No.		Material[a] Condition	Stress, Ksi	Time Hrs.	% Elong.	% R of A
17-1	2562 + 6 v/o	RR, 20%	6.5	16.1	5.6	14.5
17-2	2562 + 6 v/o	RR, 20%	6.5	24.1	Load increased	
			7.0	68.1		
			7.5	26.1		
			8.0	23.7		
			8.5	24.4		
			9.0	1.3	7.0	22.3
17-3	2562 + 6 v/o	RR, 20%	6.5	45.4	Load increased	
			7.0	26.6		
			7.5	24.2		
			8.0	24.0		
			8.5	5.6		
			9.0	0.3	9.8	37.0

[a] RR = Rod Roll, % = reduction in area

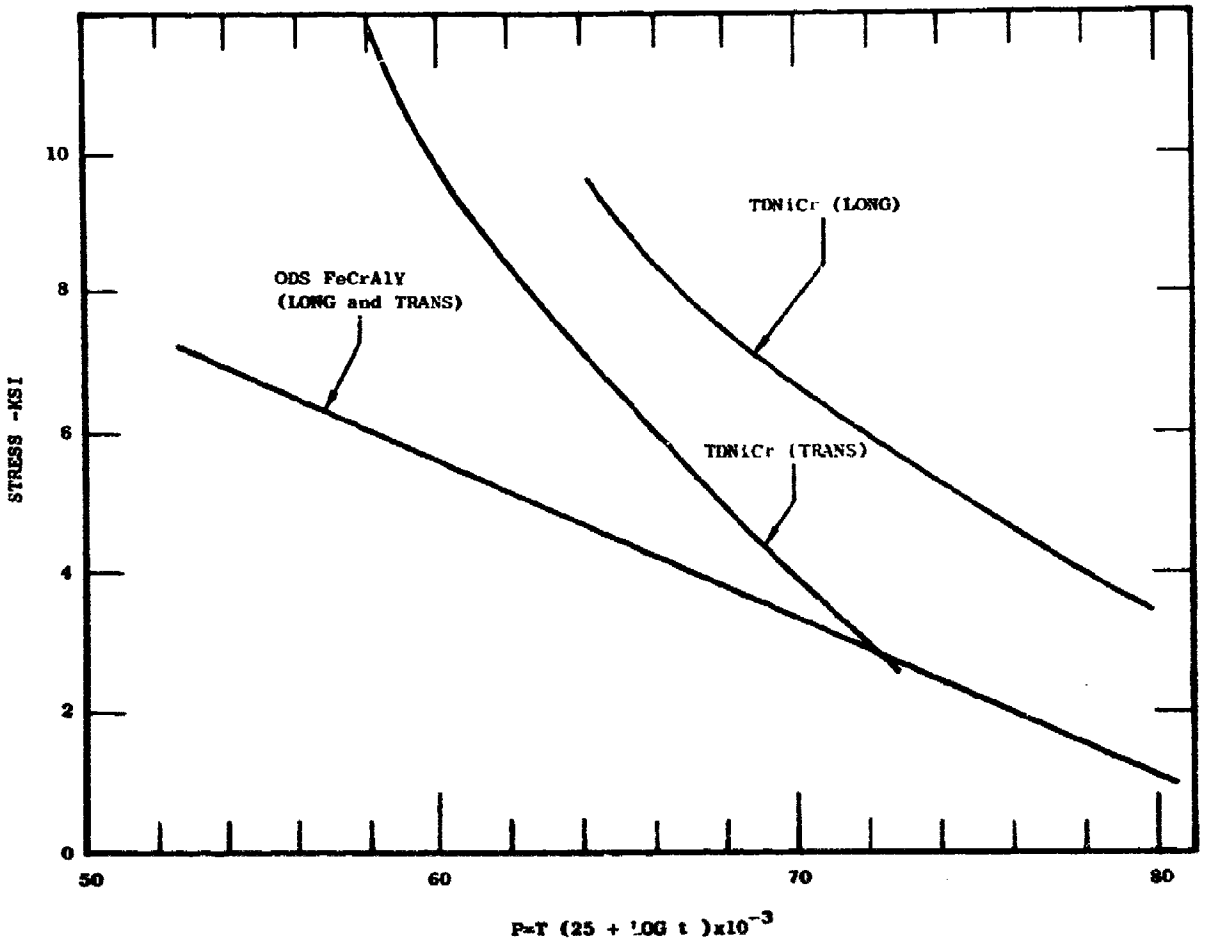

Figure 1 Rupture Stress vs Larsen Miller Parameter Showing a Comparison of TDNiCr and Alloy 1562 + 4V0 Oxide Sheet

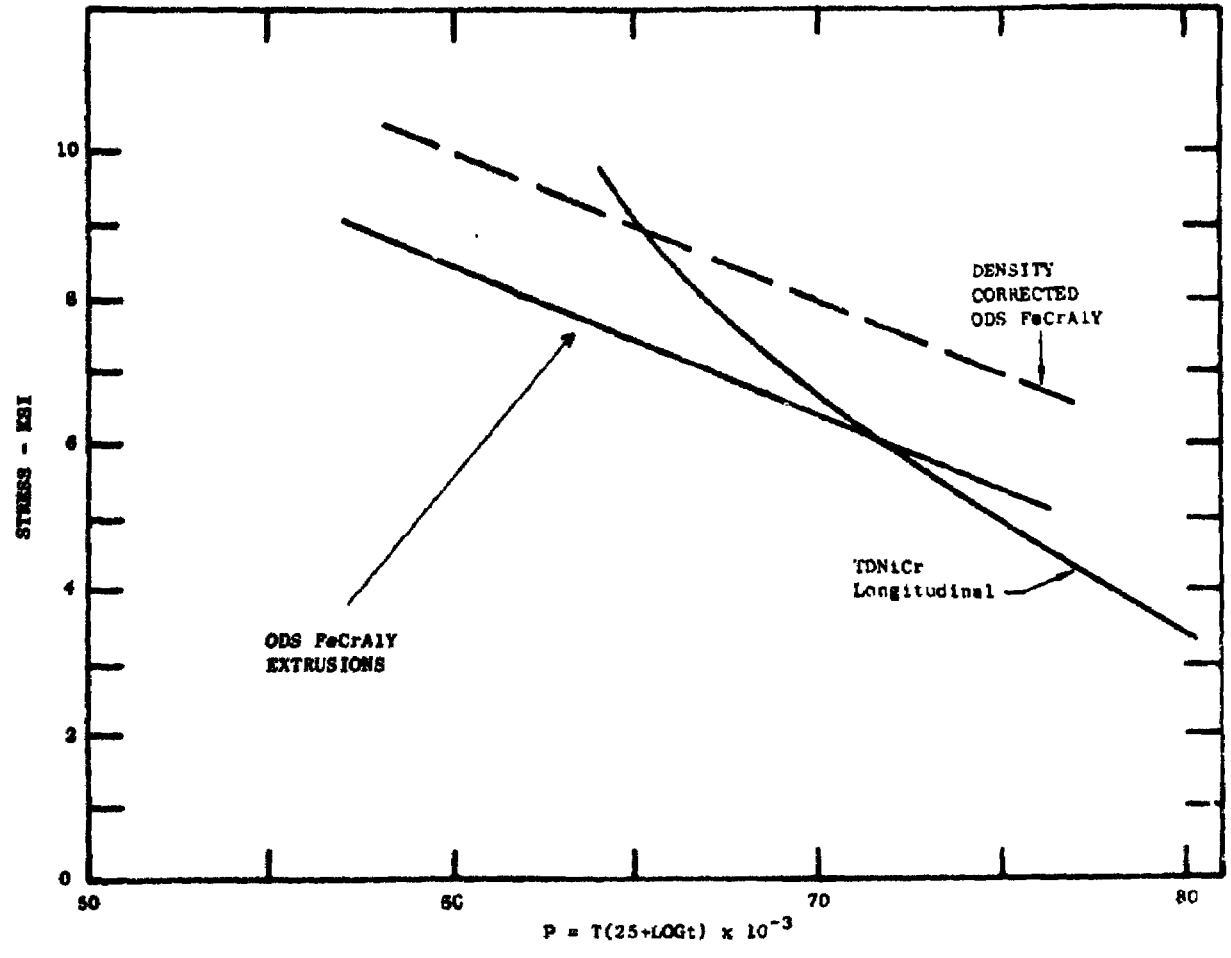

Figure 2 Longitudinal Stress Rupture Properties of ODS FeCrAlY Bar in Comparison to TDNiCr Sheet Properties. Also Shown is a Density Corrected Curve for ODS FeCrAlY Which was Obtained Using a Stress Multiplying Factor of $\frac{\text{Density TDNiCr}}{\text{Density ODS FeCrAlY}}$

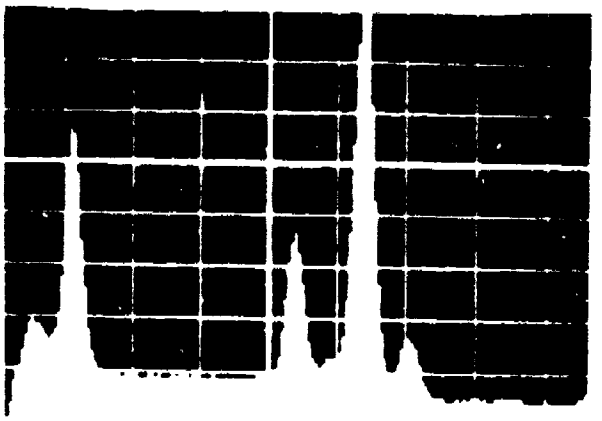

Al Au Cr Fe

2300x

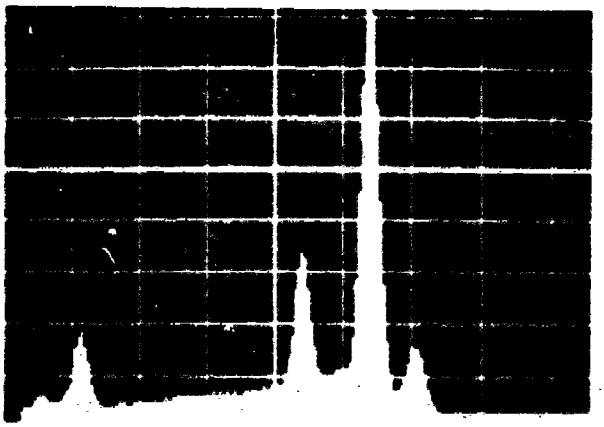

Al Au Cr Fe

Figure 3 Scanning Electron Microscope (SEM)/Energy Dispersion Analysis X-Ray (EDAX) of an Fe15Cr6Al2Y Powder Particle Showing Break-Away Oxidation at 1.2 Weight Percent Oxygen Level. Specimen Shadowed with Gold

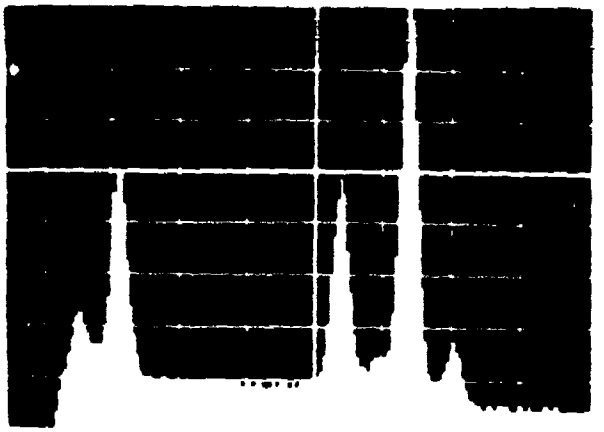

Al Au Cr Fe

2300x

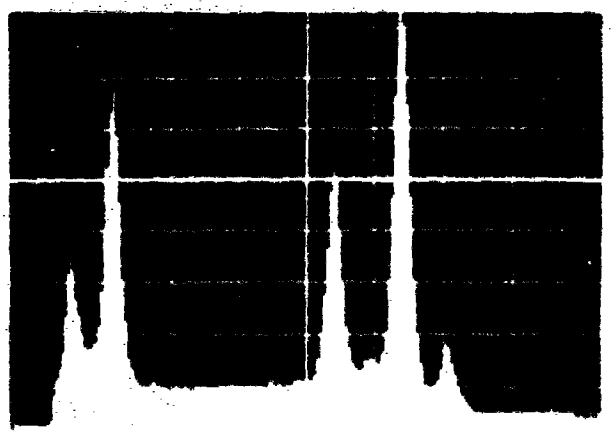

Al Au Cr Fe

Figure 4 Scanning Electron Microscope (SEM)/Energy Dispersion Analysis X-Ray (EDAX) of an Fe20Cr6Al2Y Powder Particle. No Detectable Break-Away Oxidation at 1.4 Weight Percent Oxygen Level. Specimen Shadowed with Gold

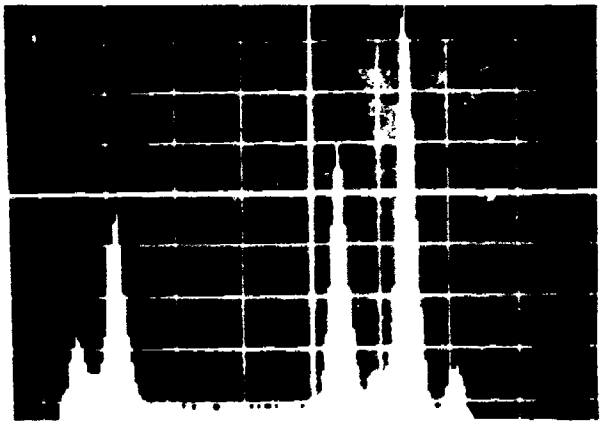

Al Au Cr Fe

2300x

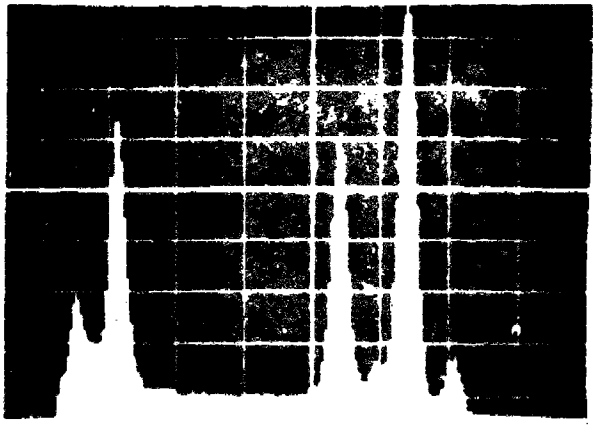

Al Au Cr Fe

Figure 5 Scanning Electron Microscope (SEM)/Energy Dispersion Analysis X-Ray (EDAX) of an Fe25Cr6Al2Y Powder Particle. No Detectable Break-Away Oxidation at 1.1 Weight Percent Oxygen Level. Specimen Shadowed with Gold

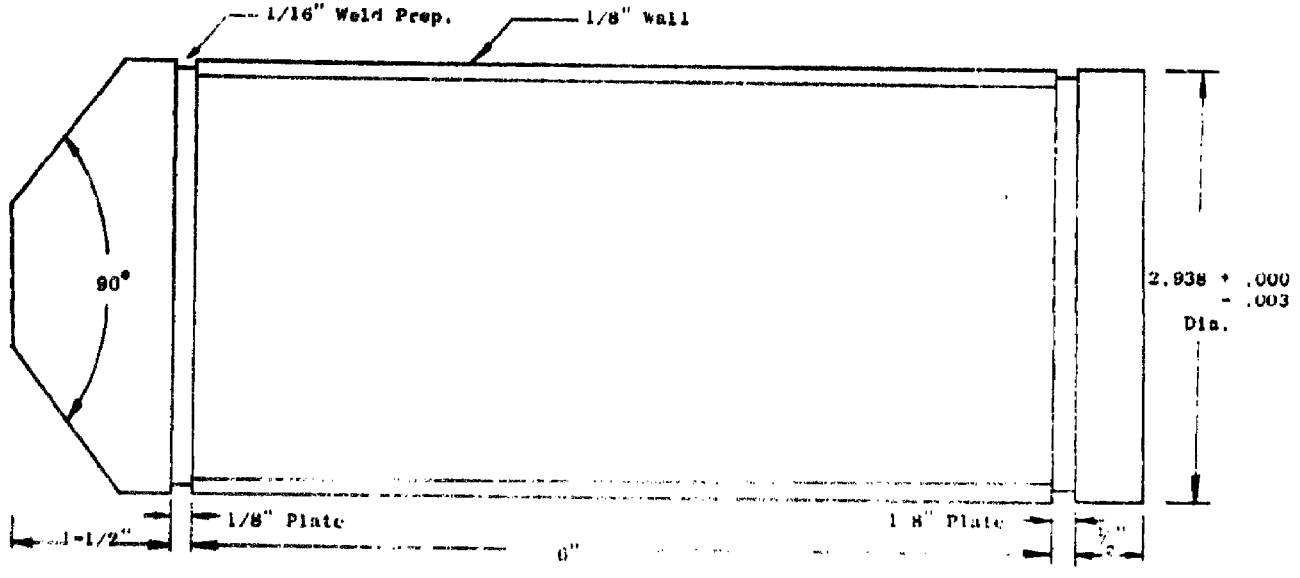

Figure 6 Extrusion Can

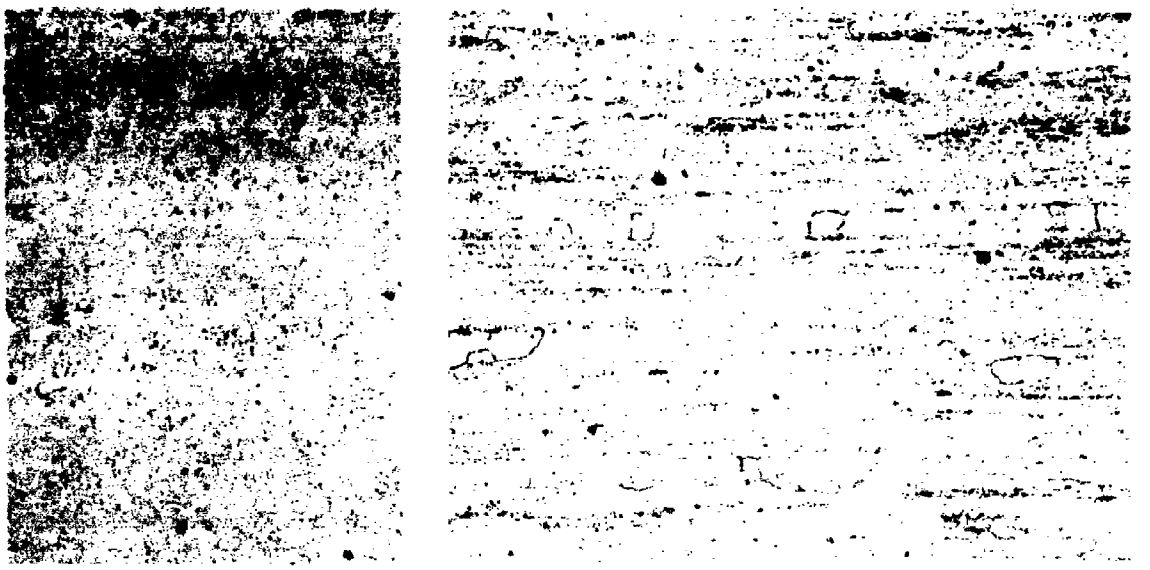

TRANSVERSE LONGITUDINAL

2562 + 4 v/o OXIDE

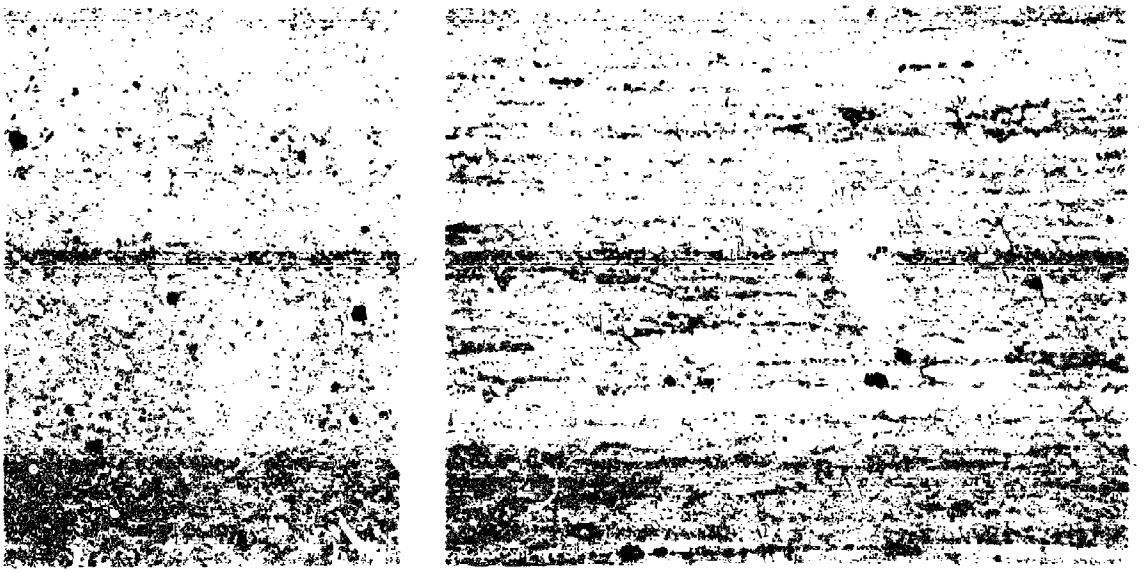

TRANSVERSE LONGITUDINAL

2062 + v/o OXIDE

Figure 7 Photomicrographs Showing (500X) Microstructure of As-Extruded Oxide Dispersion Strengthened FeCrAlY Alloys

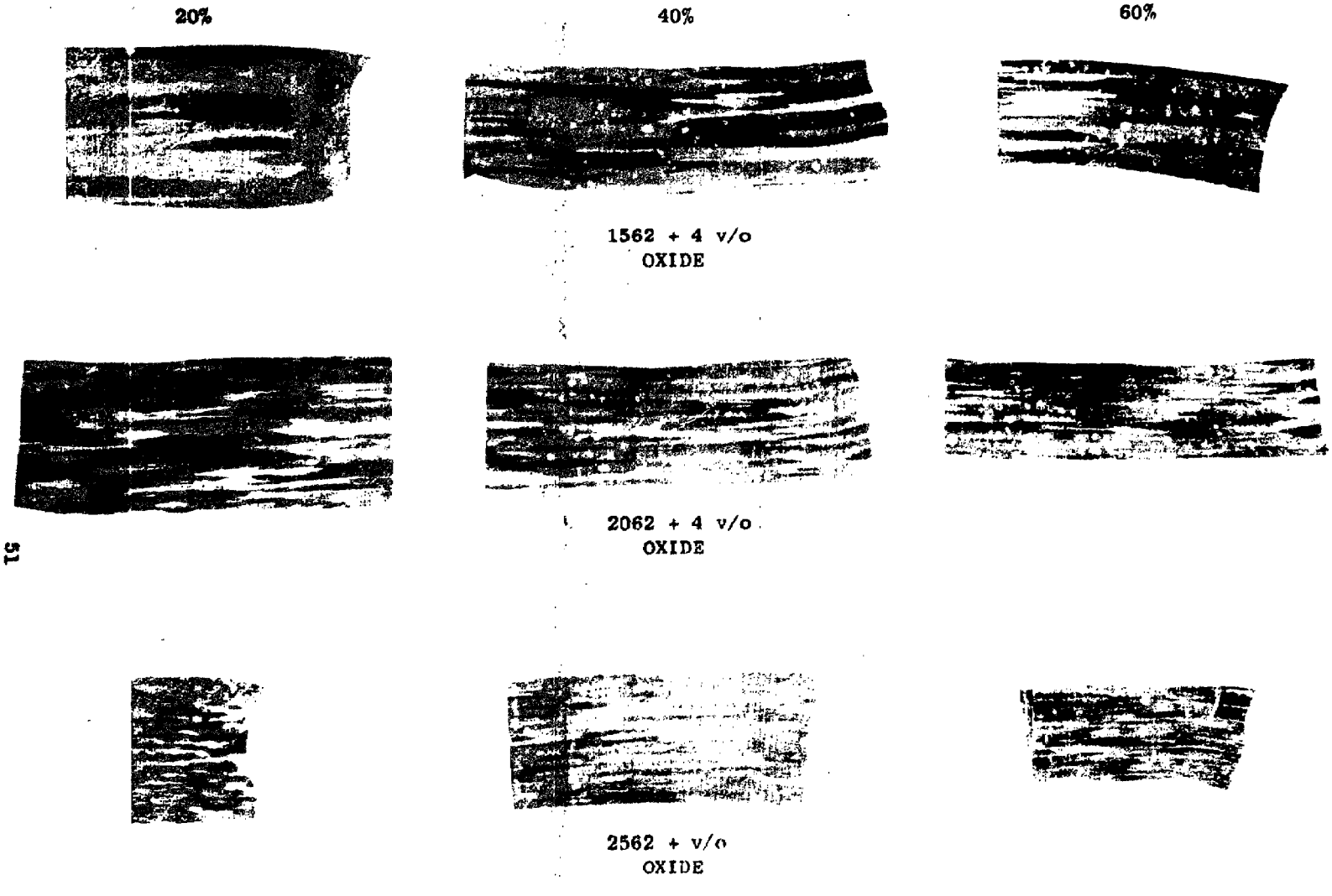

Figure 8 FeCrAlY + 4 v/o Oxide Alloys Showing the Effects of Rod Rolling at 1400°F to Various Reduction Levels Using 10% Reduction Per Pass. Furnace Recrystallized at 2400°F

2562 + 4 v/o OXIDE 2X

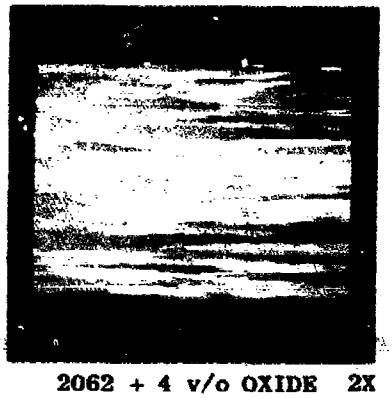

2062 + 4 v/o OXIDE 2X

Figure 9 Photomacrographs Showing the Structure of Oxide Dispersion Strengthened FeCrAlY Alloys in the Rod Rolled and Furnace Recrystallized Condition

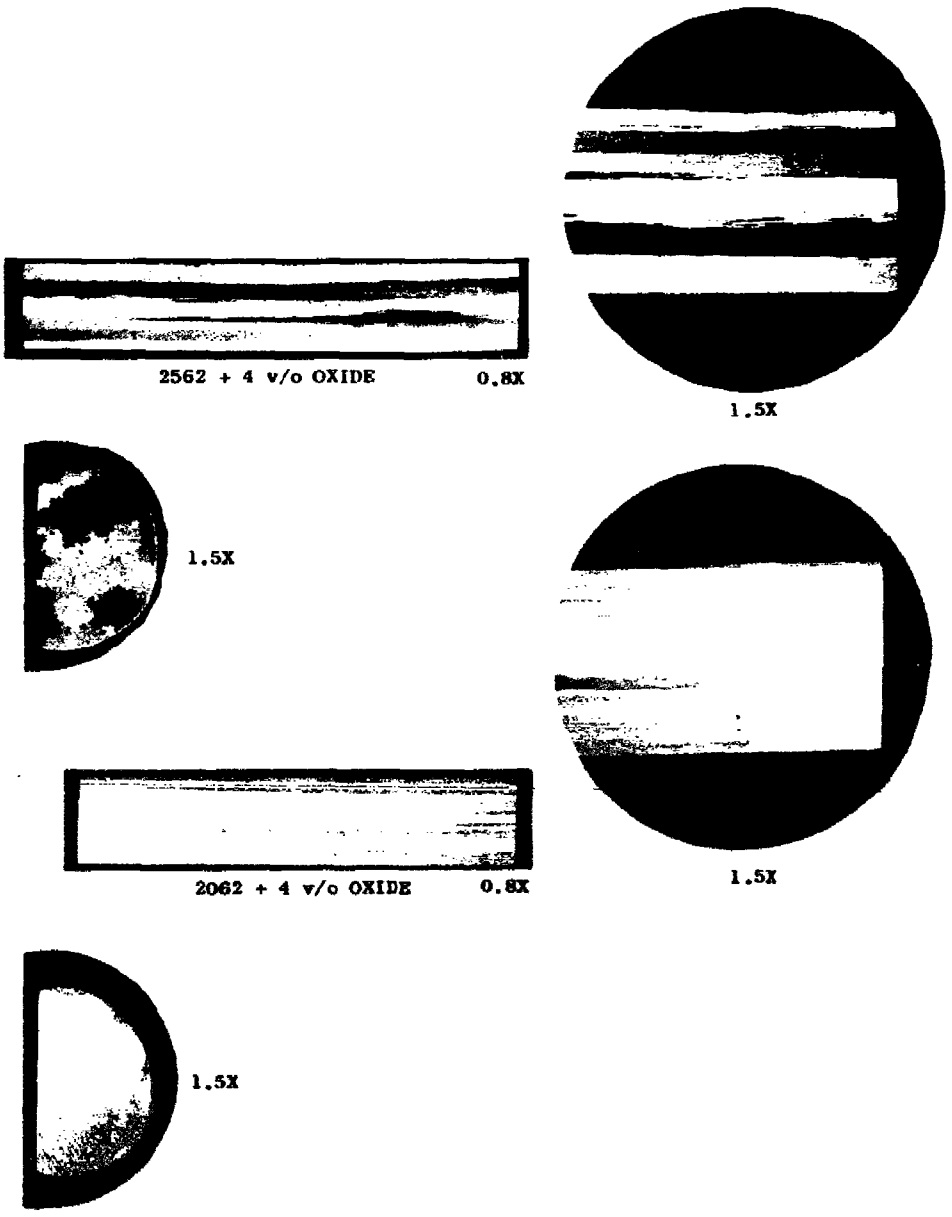

Figure 10 Photomacrographs Showing the Structure of Oxide Dispersion Strengthened FeCrAlY Alloys in the Rod Rolled and Directionally Recrystallized Condition

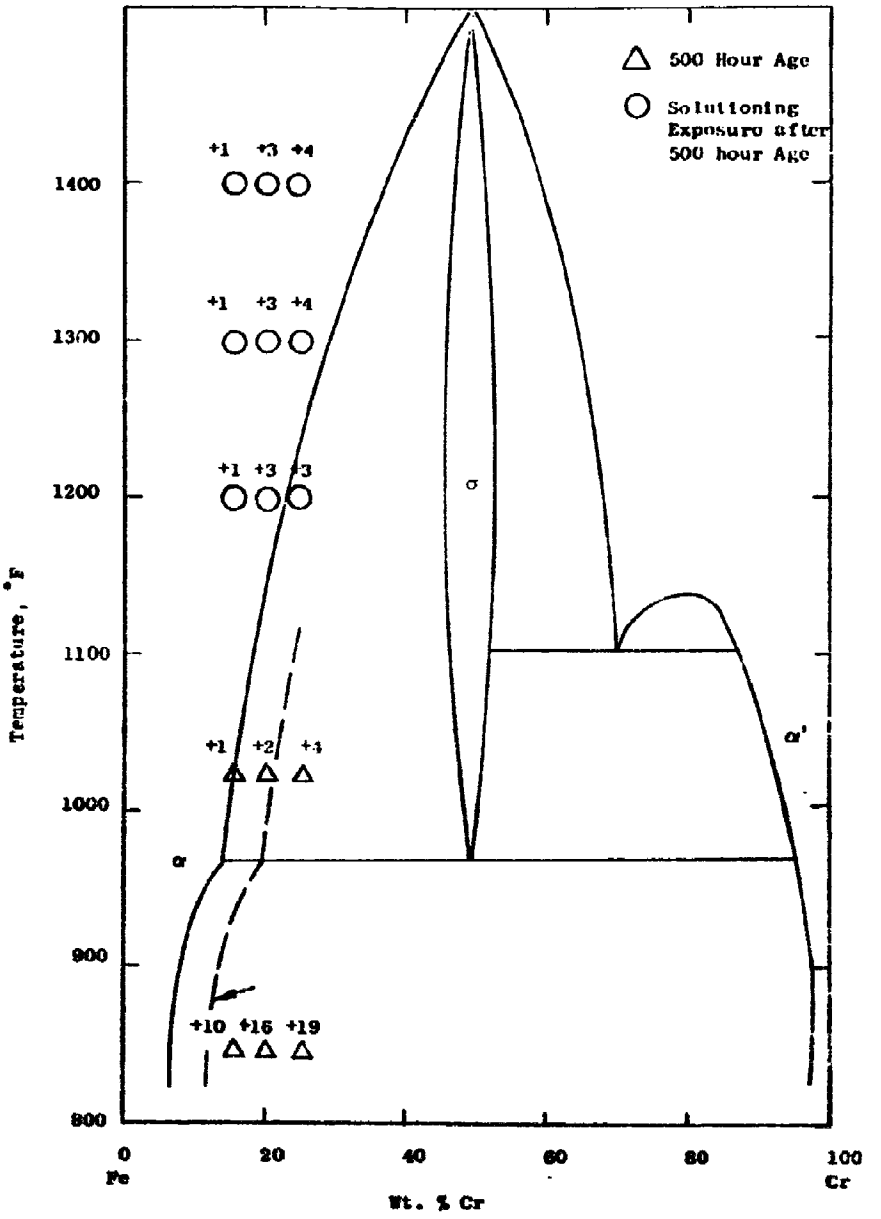

Figure 11 Fe Cr Binary Diagram Showing Estimated Psuedo-Binary α/α' + Phase Boundary for Fe, Cr - 6% Al Alloys. Aging Exposures of ODS Alloys 1562, 2062 and 2562 are shown as Triangles, While Solutioning Exposures of Material Aged at Both 842 and 1025F for 500 Hrs. are Shown as Circles. The Number Corresponding to Each Point Indicates the Increase Over Unaged Hardness associated with Each Exposure.

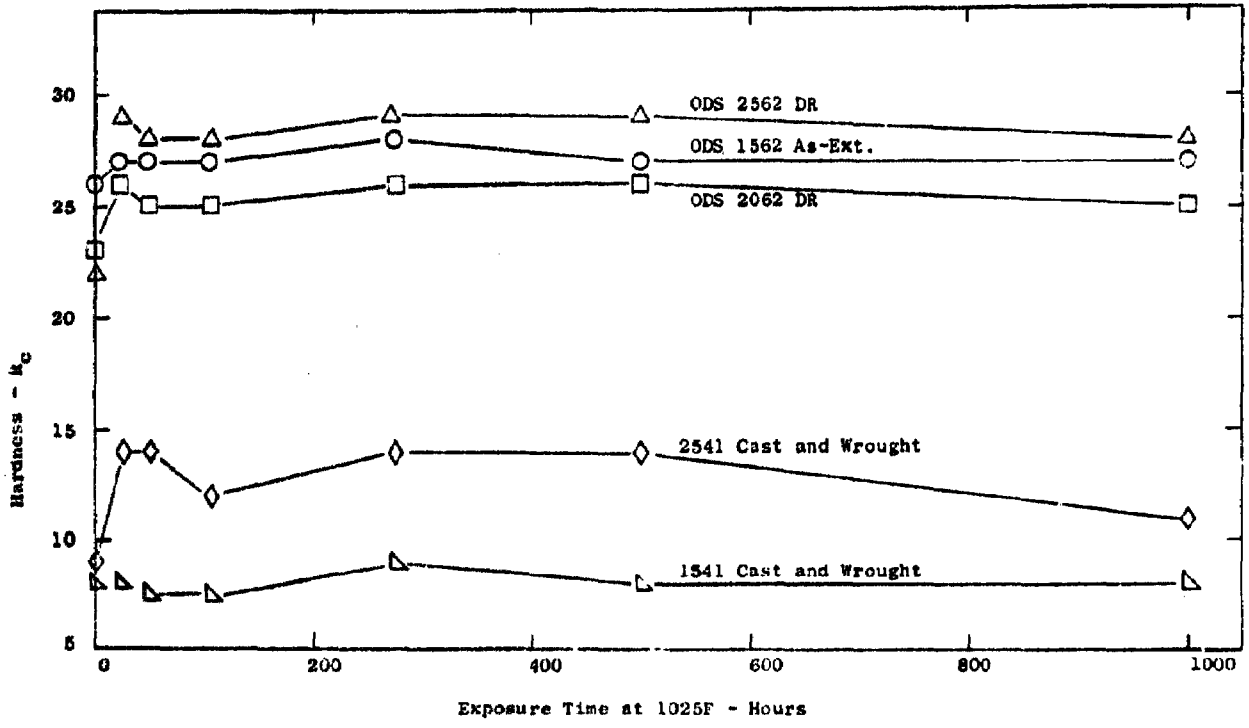

Figure 12 The Influence of 1025F Aging on Hardness of ODS Alloys 1562, 2062 and 2562 in Comparison to Hardness of Cast and Wrought Alloys 1541 and 2541

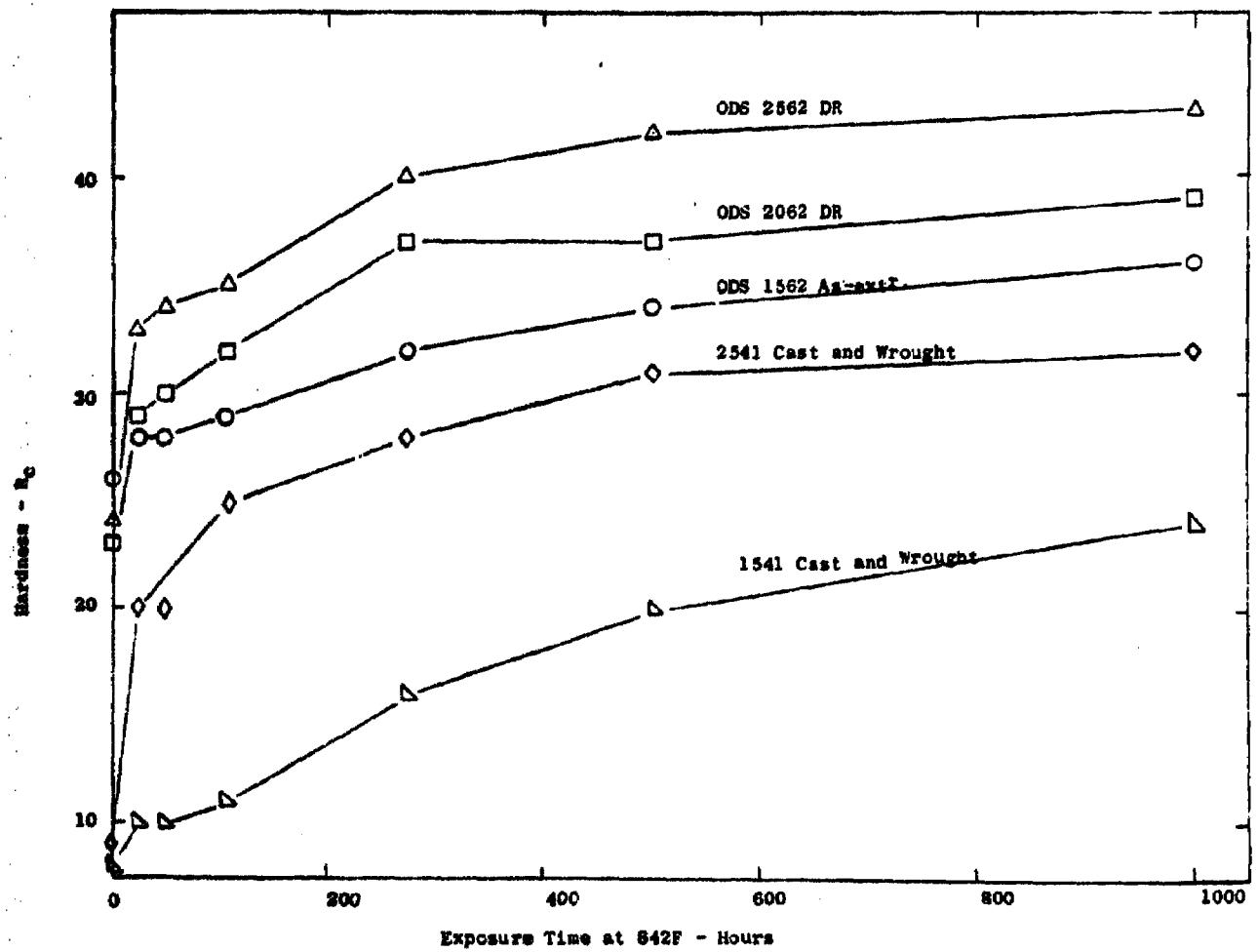

Figure 13 Hardness Changes in ODS Alloy 1562, 2062 and 2562 During Aging at 842F. Cast and Wrought Alloys 1541 and 2541 are also Included for Comparison

DIRECTIONALLY RECRYSTALLIZED 4000X

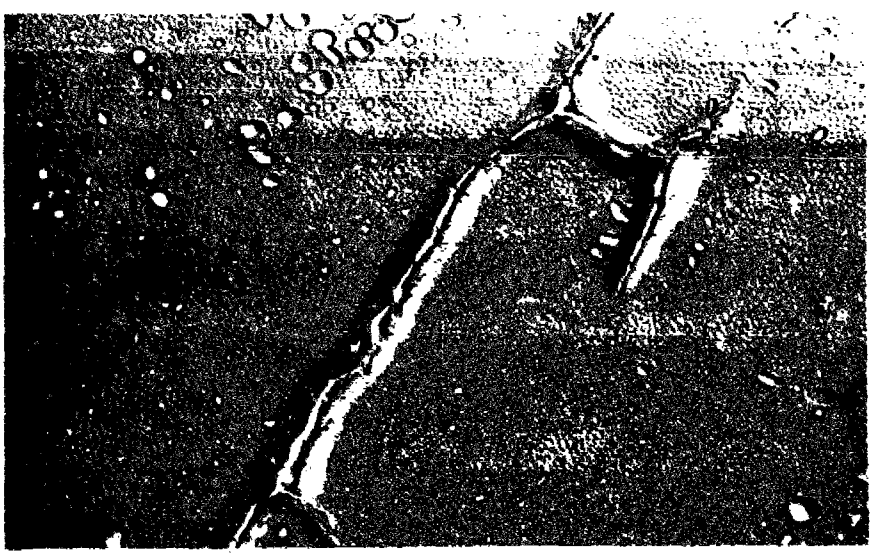

AGED AT 1025°F FOR 500 HOURS 4000X

Figure 14 Electron Photomicrographs Showing the Microstructure of 2062 + 4 v/o Oxide Alloy in the Directionally Recrystallized and Aged Condition

DIRECTIONALLY RECRYSTALLIZED 4000X

AGED AT 1025°F FOR 500 HOURS 4000X

Figure 15 Electron Photomicrographs Showing the Microstructure of 2562 + 4 v/o Oxide Alloy in the Directionally Recrystallized and Aged Condition

Figure 16 Scanning Electron Microscope (SEM)/Energy Dispersion Analysis X-ray (EDAX) of 2562 + 4 v/o Oxide Alloy Aged at 1025°F for 500 Hours. The Nearly Equi-atomic Cr and Fe Content Indicates the Precipitate to be Sigma Phase (σ)

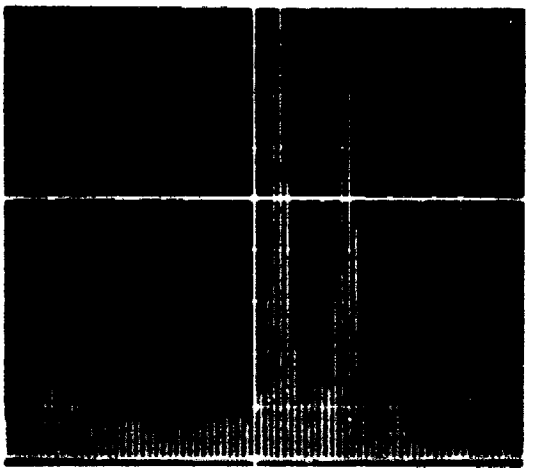

8750X

Figure 17 Scanning Electron Microscope (SEM)/Energy Dispersion Analysis X-Ray (EDAX) of 2562 + 4 v/o Oxide Alloy Aged at 1025°F for 500 Hours. The Nearly Equi-atomic Cr and Fe Content Indicates the Precipitate to be Sigma Phase (σ)

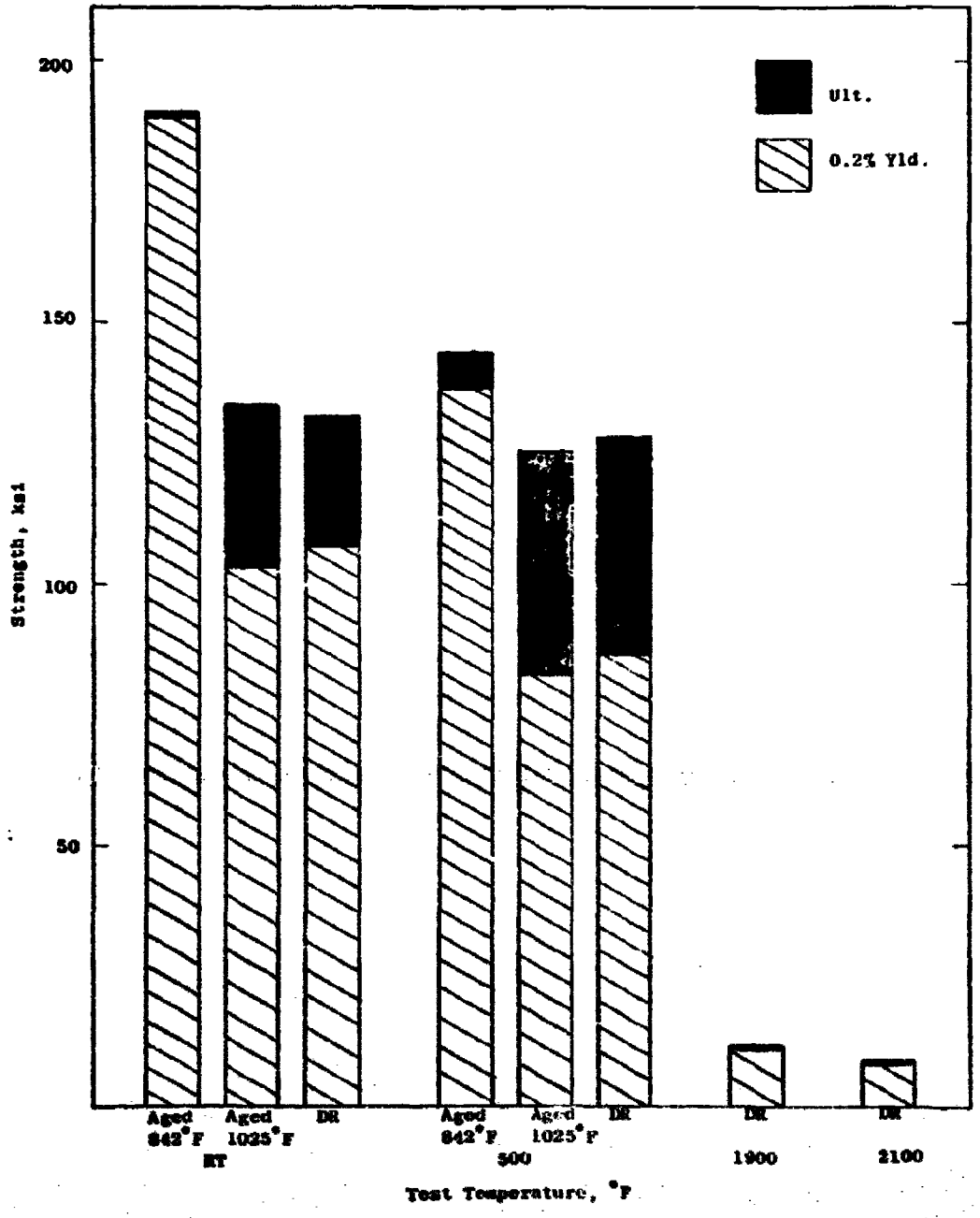

Figure 18 Tensile Properties of 2062 + 4 v/o Oxide Alloy in the Directionally Recrystallized and Aged Conditions

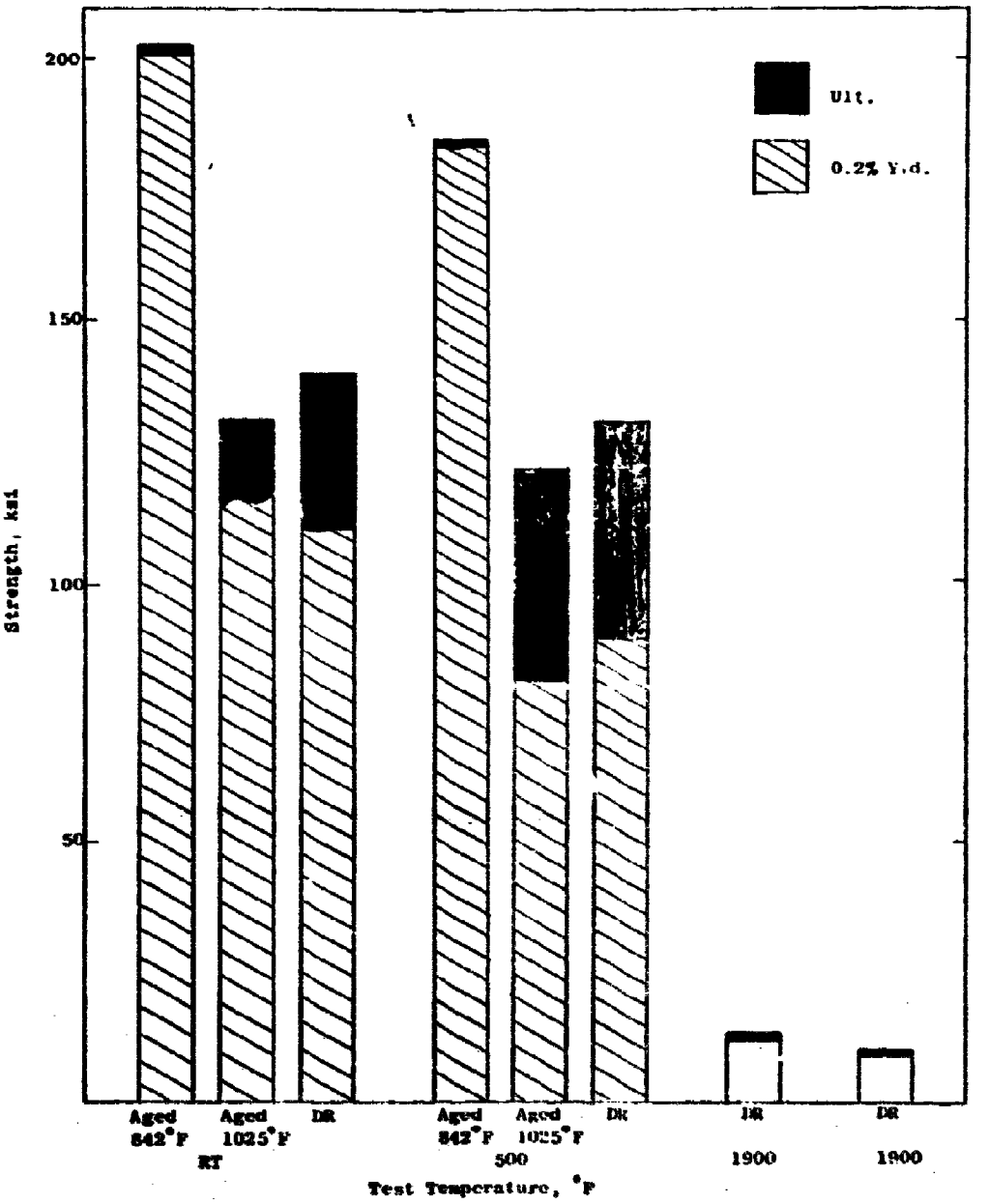

Figure 19 Tensile Properties of 2562 + 4 v/o Oxide Alloy in the Directionally Recrystallized and Aged Conditions

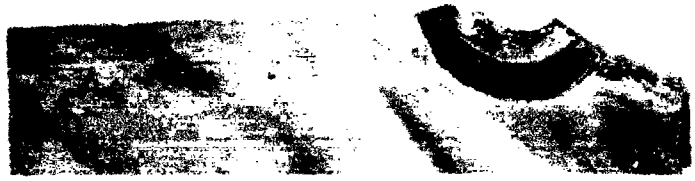

1X

Figure 20 Photograph of a 1562 + 4 v/o Oxide Alloy .060" Thick Sheet Specimen Showing "Breakaway" Oxidation After a 2400°F Exposure in Air for 100 Hours

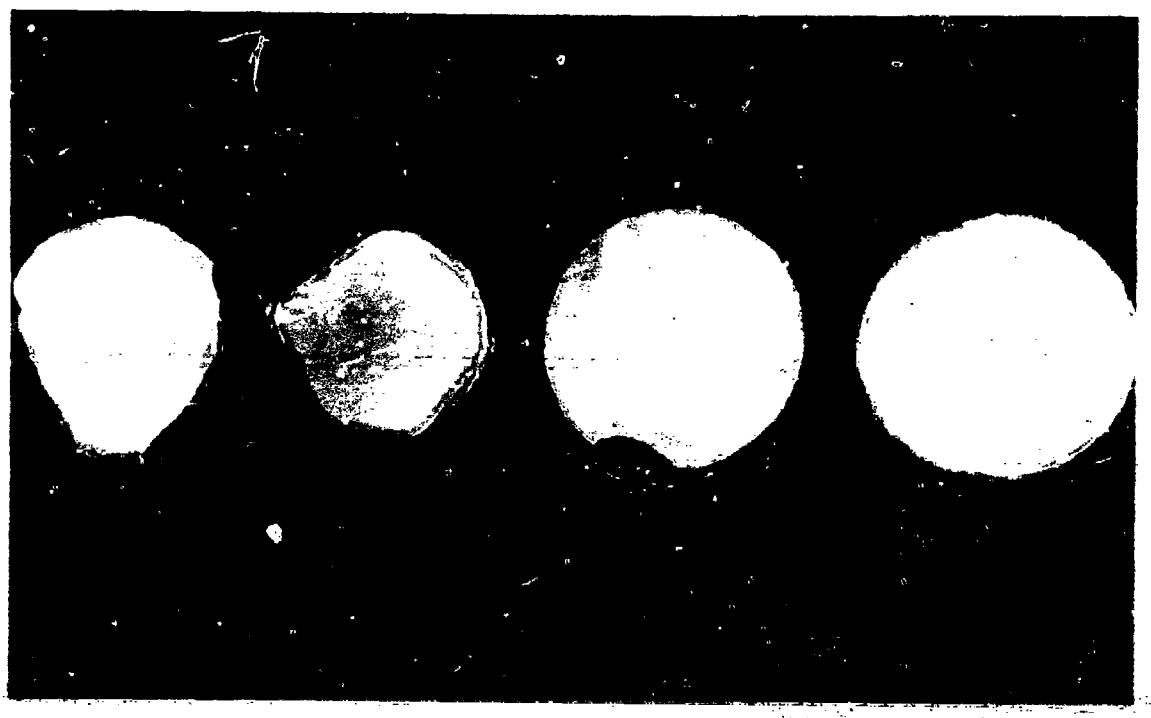

1562 + 4 v/o 1562 + 4 v/o 2062 + 4 v/o 2562 + 4 v/o

Figure 21 Photomacrographs of Oxide Dispersion Strengthened FeCrAlY Alloy Showing Resistance to "Breakaway" Oxidation Subsequent an Exposure at 2400°F in Air for 70 Hours. The Extruded Segments Were Left in the Mild Steel Extrusion Jacket to Initiate a Catastrophic Oxidation Rate and Test the Alloys Healing Ability 3X

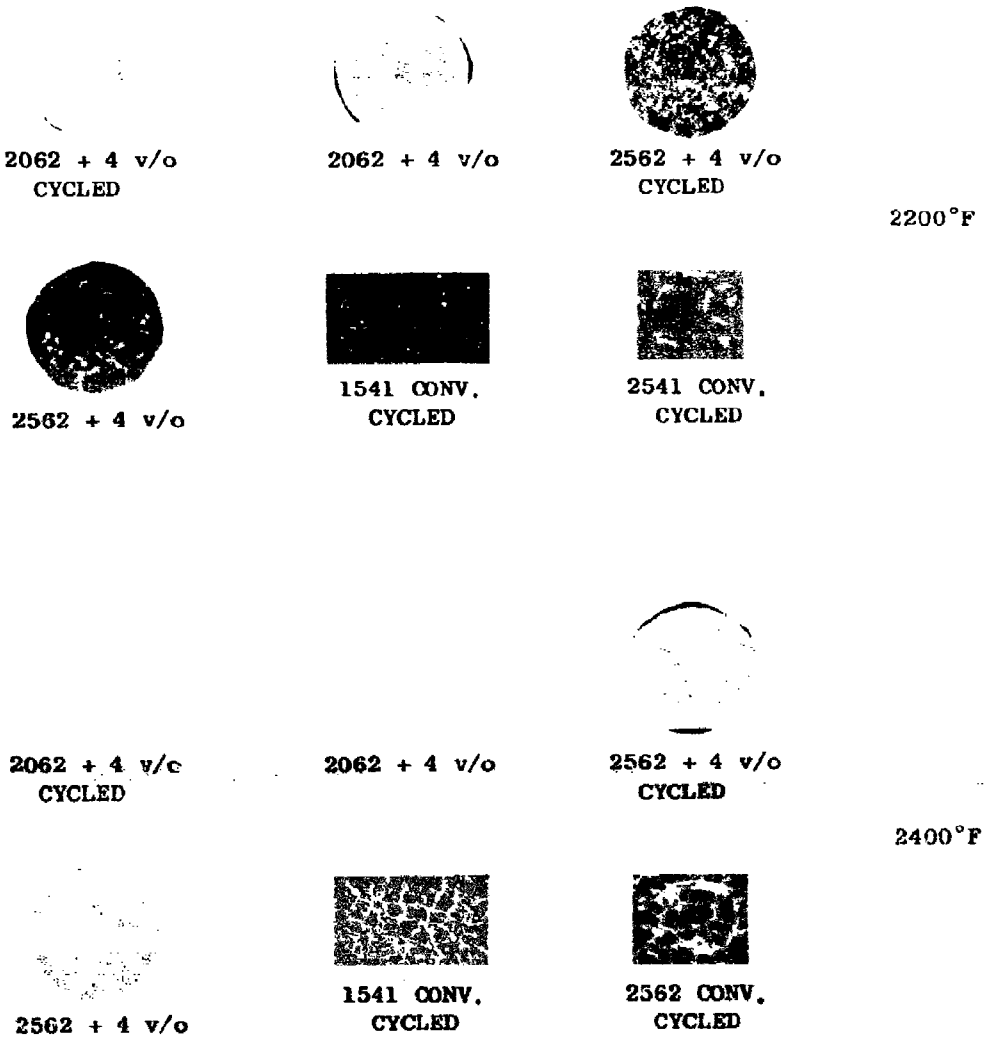

Figure 22 Photomacrographs (1.5 X) Showing the Oxidation Resistance of Oxide Dispersion Strengthened FeCrAlY Alloys in Comparison to Conventional Cast and Wrought Alloys. Furnace Exposures Were at 2200° and 2400°F in Air for 500 Hours.

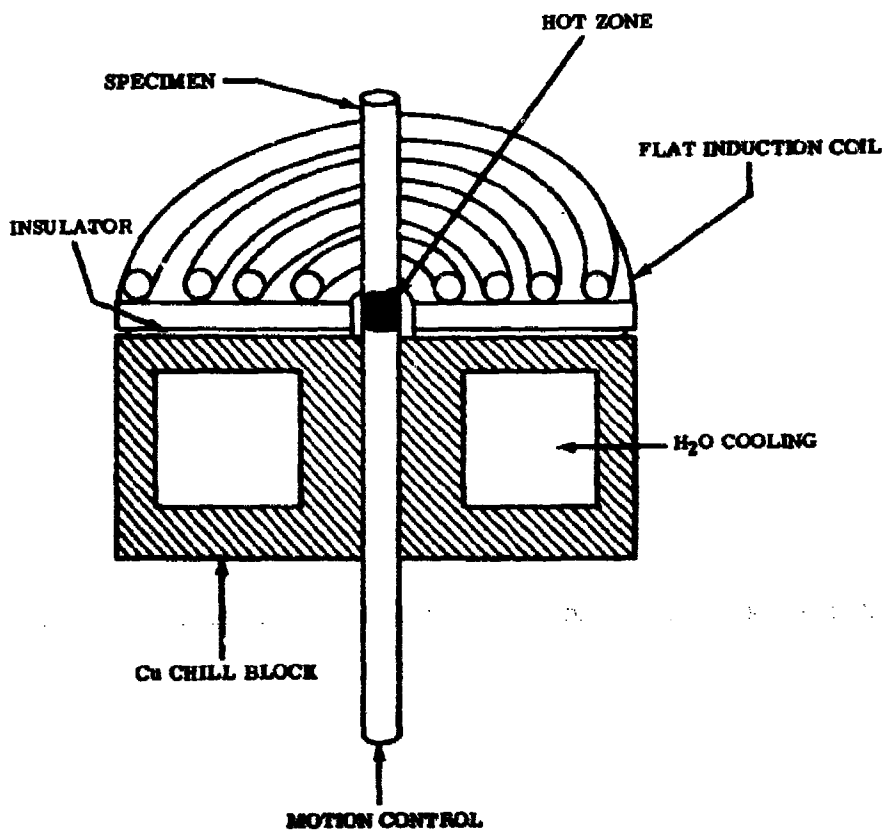

Figure 23 Schematic Diagram of Induction Coil Heat Source and Water Cooled Copper Chill Block Combinations Used to Produce Elongated Microstructures in the DR Process

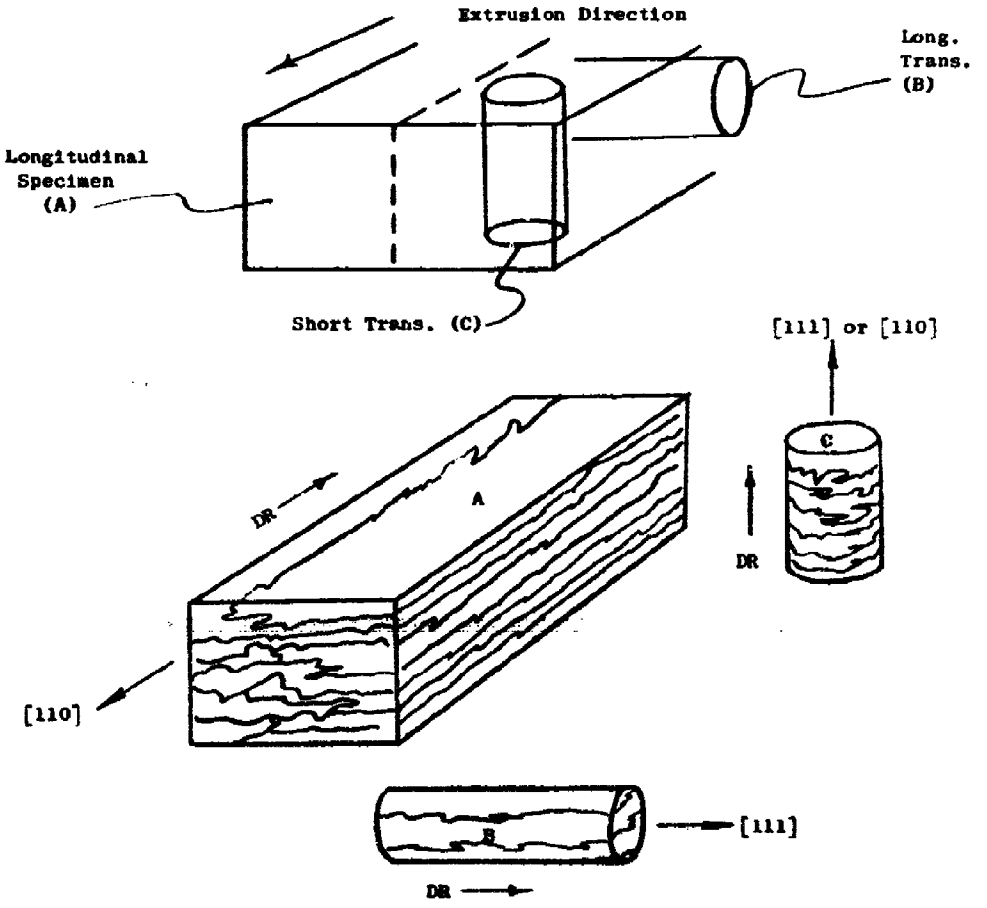

Figure 24 Orientation and Shape of DR Specimen Relative to Extrusion Direction (top) Microstructures Achieved When DR Processed in Direction of Arrows (bottom)

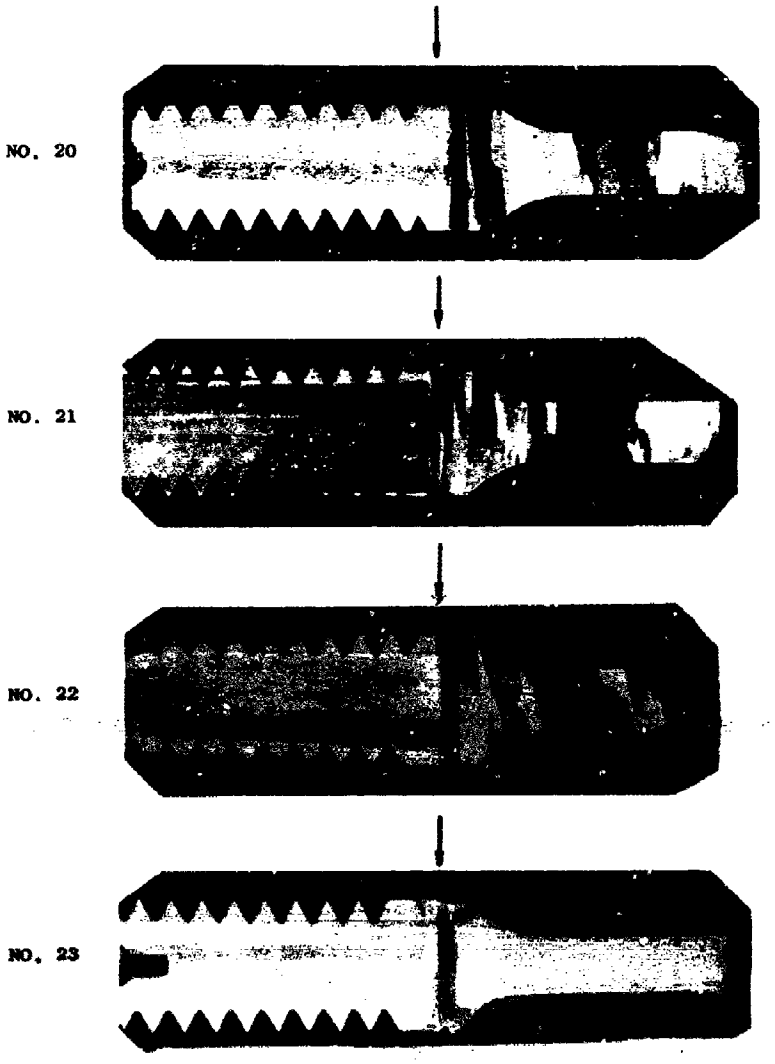

Figure 25 Photomacrographs (4X) of 1562 + 4% Oxide Alloy Stress Rupture Specimens which were Directionally Recrystallized in the Short Transverse Direction. The Braze Joined Specimens Were Ground Longitudinally and are Shown in the Macro-etched Condition. The Location of the Braze Joints are Indicated by the Arrows

NO. 25

LONG TRANSVERSE 5X

NO. 4

LONGITUDINAL 6.5X

Figure 26 Photomacrographs of 1562 + 4 v/o Oxide Alloy Stress-Rupture Specimens. Specimen No. 25 was Directionally Recrystallized in the Long Transverse Direction. Specimen No. 4 was a Furnace Recrystallized Longitudinal Specimen.

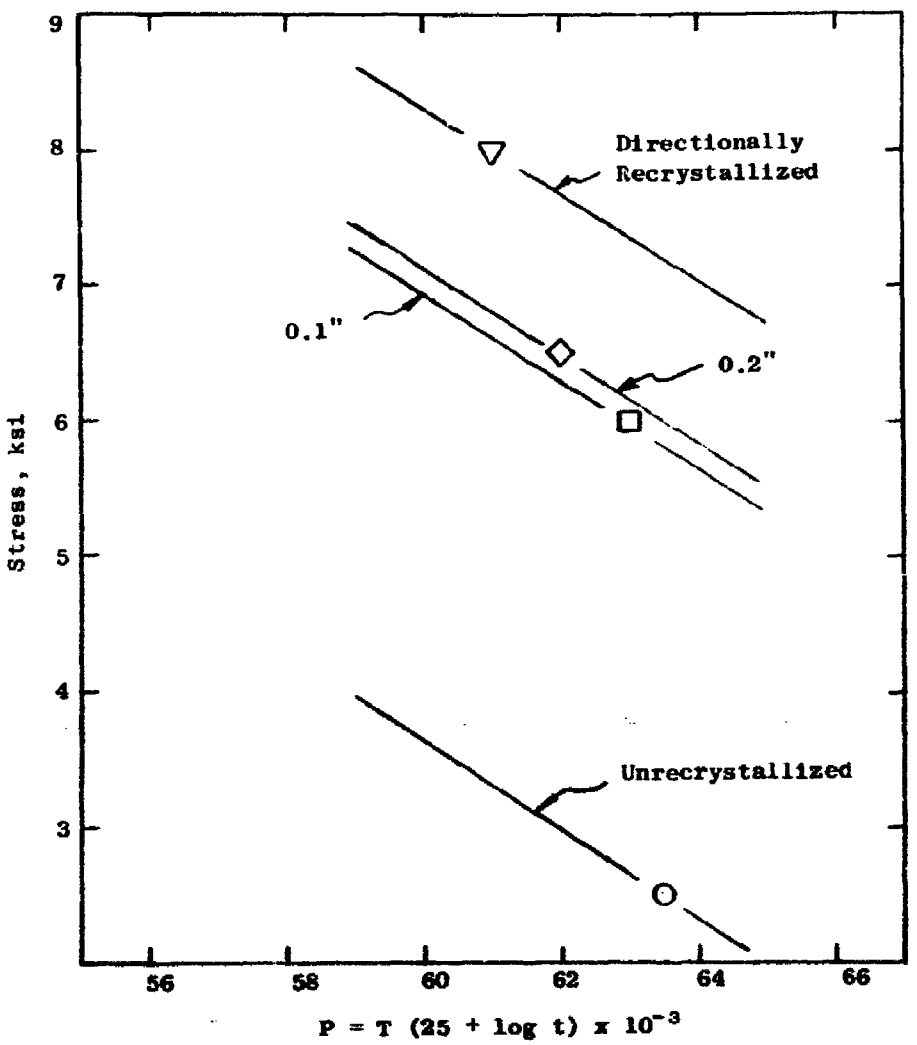

Figure 27 Larsen Miller Plot Showing the Effect of Grain Size on the Rupture Strength of Oxide Dispersion Strengthened FeCrAlY Alloys

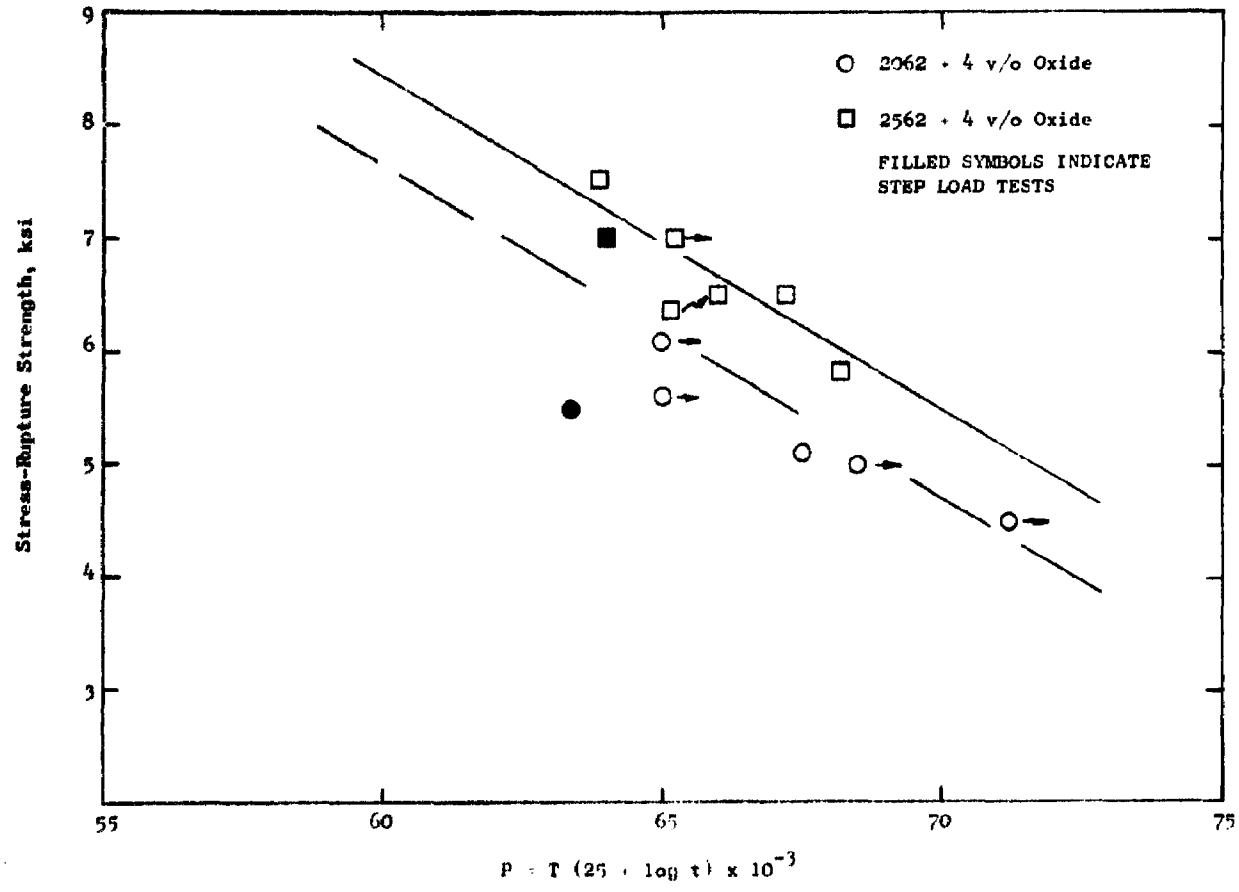

Figure 28 Larson Miller Plot Showing the Stress-Rupture Strengths of Oxide Dispersion Strengthened FeCrAlY Alloys

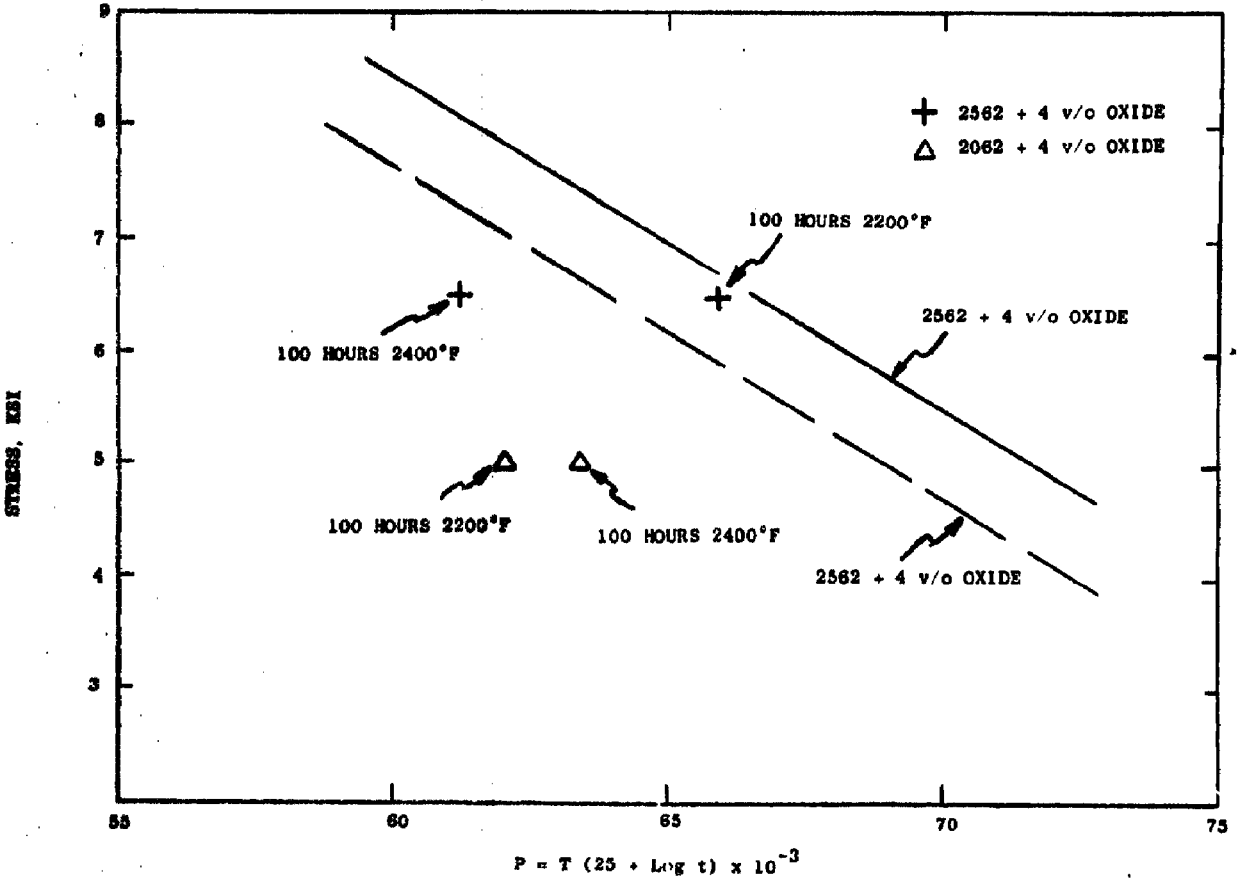

Figure 29 Larson Miller Plot Showing the Effects of Long Time High Temperature Exposures on the Stress-Rupture Strengths of Oxide Dispersion Strengthened FeCrAlY Alloys

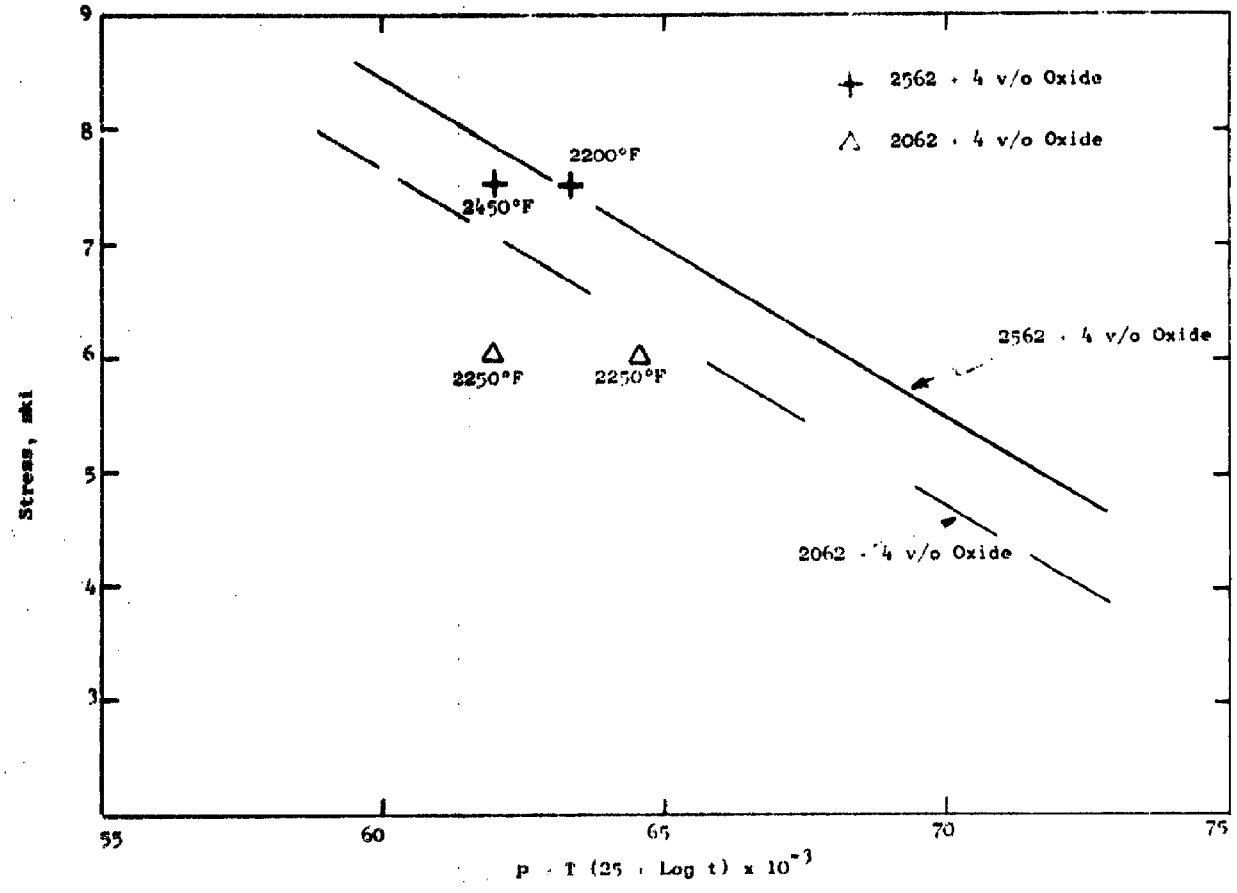

Figure 30 **Larson Miller Plot Showing the Effects of Directional Recrystallization Temperature on Oxide Dispersion Strengthened FeCrAlY Alloys**

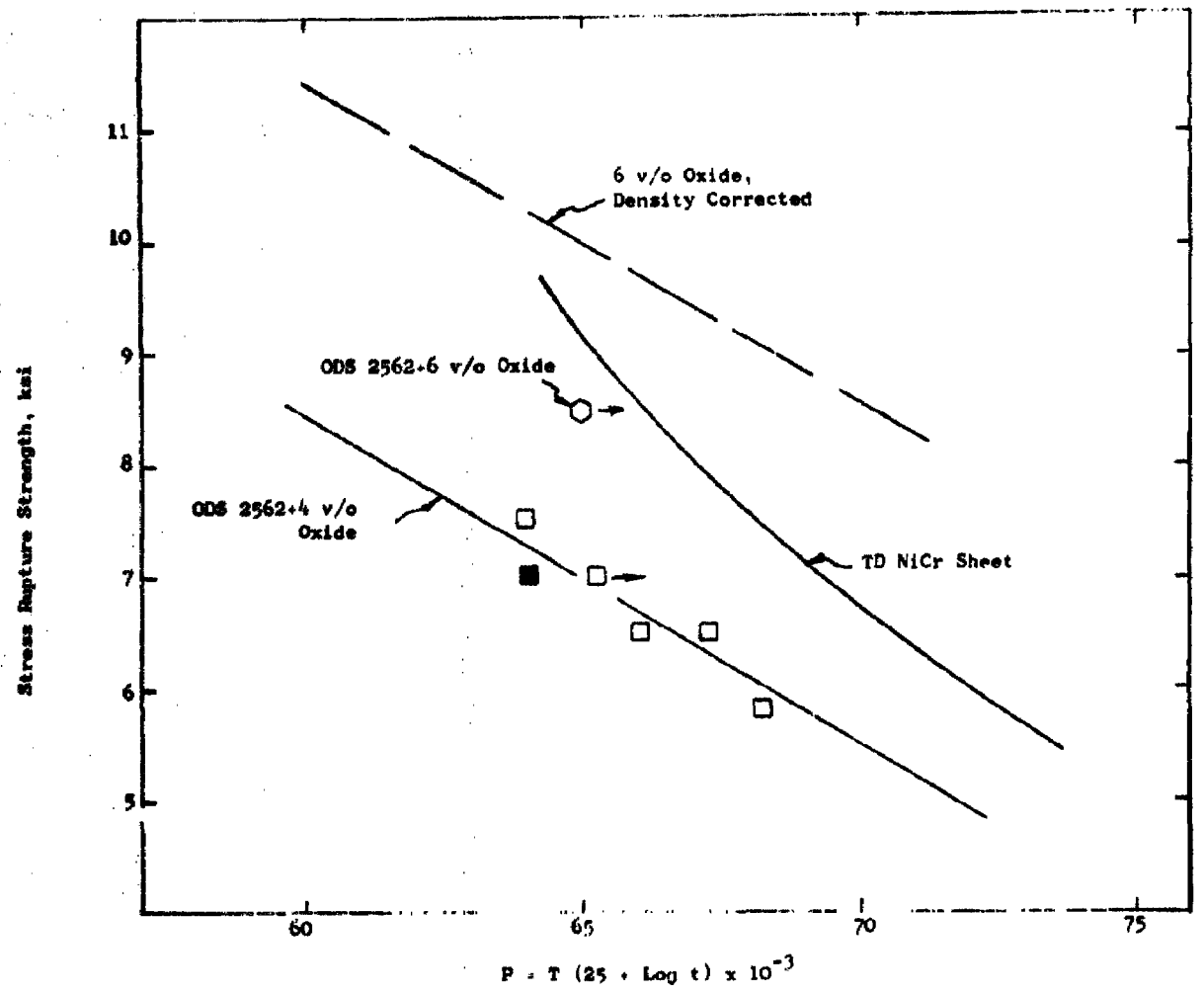

Figure 31 Larson Miller Plot Showing the Stress-Rupture Strength of 2562 + 6 v/o. Oxide Alloy Bar in Comparison to TD NiCr Sheet. Also Shown is the Density Corrected Curve for 2562 + 6 v/o Oxide Alloy Which is Obtained by Using a Stress Multiplying Factor of $\frac{\text{Density TD NiCr}}{\text{Density ODS FeCrAlY}}$

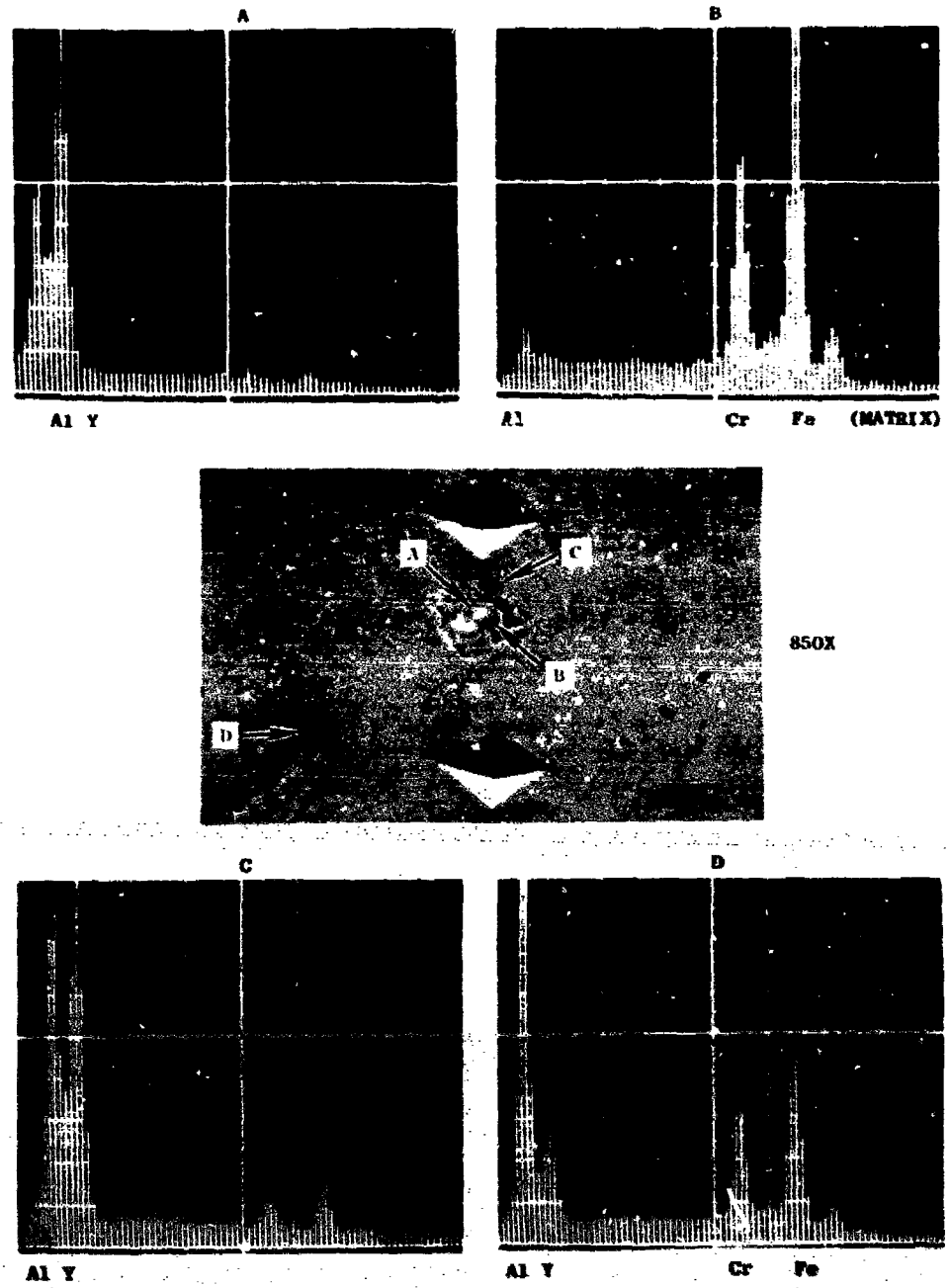

Figure 32 Scanning Electron Microscope (SEM)/Energy Dispersion Analysis X-ray (EDAX) of an 2562 + 4% Oxide Alloy Subsequent an Exposure at 2400°F for 100 Hours

DISTRIBUTION LIST
Contract N00019-72-C-0271

(One copy unless otherwise noted)

(3 copies plus balance after distribution)
U. S. Naval Air Systems Command
(AIR-52031B)
Department of the Navy
Washington, D. C. 20360

(7 copies, for internal distribution by AIR-6043, as follows:
AIR-6043 (2 copies), AIR-536B1 (1 copy), AIR-330C (1 copy) AIR-330E (1 copy), AIR-5361A (1 copy), AIR-5362A (1 copy)
U. S. Naval Air Systems Command
AIR-6043 (5 copies)
Department of the Navy
Washington, D. C. 20360

Commander
Naval Air Development Center
(Code VTM)
Warminster, Pennsylvania 18974

(2 copies)
U. S. Naval Air Turbine Test Station
Attn: E. Lister (AT-1P) (1 copy) A. Martino AT-1 (1 copy)
1440 Parkway Avenue
Trenton, New Jersey 08628

U. S. Naval Ordnance Systems Command
(ORD-33)
Department of the Navy
Washington, D. C. 20360

Commander
Naval Weapons Center
Code 5516
China Lake, California 93555

U. S. Naval Ships Systems Command
(Code 0342)
Department of the Navy
Washington, D. C. 20360

U. S. Naval Ships Research and Development Center
(Code 2612)
Annapolis, Maryland 21402

Commander Naval Ordnance Laboratory
(Metallurgy Division)
White Oak
Silver Spring, Maryland 20910

(2 copies)
Director
Naval Research Laboratory
(Code 6130 - (1 copy))
(Code 6340 - (1 copy))
Washington, D. C. 20390

Office of Naval Research
The Metallurgy Program, Code 471
Arlington, Virginia 22217

Director
Army Materials and Mechanics Research Center
(A. Gorum)
Watertown, Massachusetts 02172

Army Materiel Command
Building T-7 Gravelly Point
Washington, D. C. 20315
ATTN: AMCRD-TC

(2 copies)
Air Force Materials Laboratory
(Code LL - H. M. Burte)
Wright-Patterson Air Force Base
Ohio 45433

National Aeronautics and Space Administration
(Code RWM)
Washington, D. C. 20546

(2 copies)
National Aeronautics and Space Administration
Lewis Research Center
(G. M. Ault - (1 copy))
(H. P. Probst - (1 copy))
21000 Brookpark Road
Cleveland, Ohio 44135

U. S. Atomic Energy Commission
Division of Reactor Development
(A. Van Echo)
Washington, D. C. 20545

Metals and Ceramics Information Center
Battelle Memorial Institute
505 King Avenue
Columbus, Ohio 43201

The Johns Hopkins University
Applied Physics Laboratory
(Maynard L. Hill)
8621 Georgia Avenue
Silver Spring, Maryland 20910

AVCO RAD
201 Lowell Street
Wilmington, Massachusetts 01887

IIT Research Institute
10 West 35th Street
Chicago, Illinois 60616

Detroit Diesel Allison Division
General Motors Corporation
Materials Laboratories
Indianapolis, Indiana 46206

Pratt and Whitney Aircraft Division
United Aircraft Corporation
East Hartford, Connecticut 06108

United Aircraft Research Labs
United Aircraft Co.
East Hartford, Connecticut 06108

Airesearch Division
Garrett Corporation
Phoenix, Arizona 85001

Lycoming Division
AVCO Corporation
Stratford, Connecticut 06497

Curtis Wright Company
Wright Aeronautical Division
Wood-Ridge, New Jersey 07075

Bell Aerosystems Company
Technical Library
P. O. Box 1
Buffalo, New York 14240

General Electric Company
Aircraft Engine Group
Materials and Processes Technology Laboratories
Evendale, Ohio 45215

Solar
(Dr. A. Metcalfe)
2200 Pacific Highway
San Diego, California 92112

Teledyne CAE
1330 Laskey Road
Toledo, Ohio 43601

Stellite Division
Cabot Company
Technical Library
P. O. Box 746
Kokomo, Indiana 46901

Crucible Inc.
Materials Group
P. O. Box 88
Pittsburgh, Pa. 15230
Attn: Mr. E. J. Dulis

Fansteel Inc.
Metals Division
5101 Tantalum Place
Baltimore, Md. 21226
Attn: Dr. L. J. Klingler

TRW Equipment Laboratories
23555 Euclid Avenue
Cleveland, Ohio 44117

Final Report Only - (12 copies)
Defense Documentation Center
Cameron Station
Alexandria, Virginia 22314
Via: Commander, Naval Air Systems Command (AIR-604A1)
Department of the Navy
Washington, D. C. 20360

Security Classification

DOCUMENT CONTROL DATA - R & D

(Security classification of title, body of abstract and indexing annotation must be entered when the overall report is classified)

1. ORIGINATING ACTIVITY (Corporate author)
Materials and Process Technology Labs., Aircraft Engine Group, General Electric Co., Evendale, Ohio

2a. REPORT SECURITY CLASSIFICATION
Unclassified

2b. GROUP

3. REPORT TITLE
Strengthening of FeCrAlY Oxidation Resistant Alloys

DISTRIBUTION LIMITED TO U.S. GOVERNMENT AGENCIES ONLY;
☐ FOREIGN INFORMATION
☐ PROPRIETARY INFORMATION
☒ TEST AND EVALUATION
☐ CONTRACTOR PERFORMANCE EVALUATION
DATE: 7-5-73
OTHER REQUESTS FOR THIS DOCUMENT MUST BE REFERRED TO COMMANDER, NAVAL AIR SYSTEMS COMMAND, AIR-50174

4. DESCRIPTIVE NOTES (Type of report and inclusive dates)
Final 6 April 1972 to 6 April 1973

5. AUTHOR(S) (First name, middle initial, last name)
R. E. Allen and R. J. Perkins

6. REPORT DATE
May 6, 1973

7a. TOTAL NO. OF PAGES

7b. NO. OF REFS

8a. CONTRACT OR GRANT NO.
N00019-72-C-0271

b. PROJECT NO.

c.

d.

9a. ORIGINATOR'S REPORT NUMBER(S)

9b. OTHER REPORT NO(S) (Any other numbers that may be assigned this report)

10. DISTRIBUTION STATEMENT
Distribution limited to U.S. Government Agencies only; test and evaluation, 3 May 1973. Other requests for this document must be reffered to the Commander, Naval Air Systems Command, AIR-50174

11. SUPPLEMENTARY NOTES

12. SPONSORING MILITARY ACTIVITY
Department of Navy, Navy Air Systems Command, Washington, D.C. 20360

13. ABSTRACT

An investigation of oxide dispersion strengthening (ODS) of oxidation resistant FeCrAlY alloys was conducted using argon atomized prealloyed powders and a modified SAP technique. The main objectives were to: improve surface stability; establish uniform powder pre-oxidation techniques; and improve the stress-rupture properties to the level exhibited by TD NiCr sheet. Increased chromium content proved very successful in eliminating "breakaway" oxidation. Several powder pre-oxidation techniques were identified which provide uniform oxidation and prevention of nitrogen contamination. Target weight gains were consistently achieved. Rupture stress of the ODS FeCrAlY bar was raised to the 9.0 ksi level through the addition of 6 v/o oxide and is now comparable in strength to TD NiCr at temperatures above 2000F. If a density correction is applied to the rupture stress, ODS FeCrAlY is superior to TD NiCr at temperatures above approximately 1800F.

DD FORM 1473

Unclassified

KEY WORDS	LINK A		LINK B		LINK C	
	ROLE	WT	ROLE	WT	ROLE	WT
Oxidation Resistant FeCrAlY Alloys						
Oxide Dispersion Strengthening						